A selfish DNA element engages a meiosis-specific motor and telomeres for germ-line propagation

Soumitra Sau,[1] Michael N. Conrad,[2] Chih-Ying Lee,[2] David B. Kaback,[3] Michael E. Dresser,[2] and Makkuni Jayaram[1]

[1]Department of Molecular Biosciences, University of Texas at Austin, Austin, TX 78712
[2]Program in Cell Cycle and Cancer Biology, Oklahoma Medical Research Foundation, Oklahoma City, OK 73104
[3]Department of Microbiology and Molecular Genetics, Rutgers New Jersey Medical School, Newark, NJ 07101

THE JOURNAL OF CELL BIOLOGY

The chromosome-like mitotic stability of the yeast 2 micron plasmid is conferred by the plasmid proteins Rep1-Rep2 and the cis-acting locus *STB*, likely by promoting plasmid-chromosome association and segregation by hitchhiking. Our analysis reveals that stable plasmid segregation during meiosis requires the bouquet proteins Ndj1 and Csm4. Plasmid relocalization from the nuclear interior in mitotic cells to the periphery at or proximal to telomeres rises from early meiosis to pachytene. Analogous to chromosomes, the plasmid undergoes Csm4- and Ndj1-dependent rapid prophase movements with speeds comparable to those of telomeres. Lack of Ndj1 partially disrupts plasmid–telomere association without affecting plasmid colocalization with the telomere-binding protein Rap1. The plasmid appears to engage a meiosis-specific motor that orchestrates telomere-led chromosome movements for its telomere-associated segregation during meiosis I. This hitherto uncharacterized mode of germ-line transmission by a selfish genetic element signifies a mechanistic variation within the shared theme of chromosome-coupled plasmid segregation during mitosis and meiosis.

Introduction

Meiosis is the process by which diploid nuclei undergo two distinct divisions, meiosis I and II, to form four haploid nuclei. During prophase of meiosis I, replicated homologues pair, undergo recombination, and form chiasmata, which physically link them to promote their biorientation on the metaphase spindle and subsequent anaphase separation. Meiosis II is a mitotic-like division in which sister chromatid segregation completes the production of four haploid gametes (Petronczki et al., 2003).

Meiosis in the ascomycete *Saccharomyces cerevisiae* displays the general features of meiosis in other eukaryotes, and culminates in the production of four haploid ascospores. Prophase I in *S. cerevisiae* can be divided into leptotene, zygotene, pachytene, and diplotene-like substages, as defined by the state of chromosome pairing and condensation. The sequential events that characterize these stages include clustering of perinuclear telomeres (*TEL*s) near the spindle pole body (SPB) to shape chromosomes into a bouquet, introduction of double strand DNA breaks, assembly and maturation of synaptonemal complexes (SCs), and formation, progression, and resolution of

recombination intermediates (Baker et al., 1976; Trelles-Sticken et al., 1999; Zickler and Kleckner, 1999). After dissolution of the array of cohesin complex that bridges sister chromatids from chromosome arms, but without disassembly of cohesin from centromeric regions, monopolar spindle attachment of sister chromatids and their cosegregation are ensured by the maintenance of sister kinetochore cohesion through the collaborative action of the monopolin complex, Spo13, Sgo1, and the Ipl1 kinase (Klein et al., 1999; Tóth et al., 2000; Rabitsch et al., 2003; Katis et al., 2004; Lee et al., 2004; Monje-Casas et al., 2007; Yu and Koshland, 2007). Haploidization is completed by segregation of sister centromeres (*CEN*s) during meiosis II.

An important dynamic feature of meiosis I is the manifestation of rapid prophase movements (RPMs) of chromosomes, driven presumably by cytoskeletal actin via nuclear envelope proteins (Conrad et al., 2008; Koszul et al., 2008; Wanat et al., 2008). The anchoring of *TEL*s to the envelope and bouquet formation, their attachment to the "nuclear envelope motor," and the transduction of mechanical energy from the cytoplasm to the nucleus are promoted by the Mps3-Ndj1-Csm4 (MNC) complex

Correspondence to Makkuni Jayaram: jayaram@austin.utexas.edu

Abbreviations used in this paper: *ARS*, autonomously replicating sequence; *CEN*, centromere; RPM, rapid prophase movement; SC, synaptonemal complex; *TEL*, telomere (native chromosome telomere or a telomere sequence cloned into a plasmid).

(Trelles-Sticken et al., 2005; Conrad et al., 2007, 2008; Scherthan et al., 2007; Kosaka et al., 2008; Koszul et al., 2008; Wanat et al., 2008). The accompanying *TEL*-led movements result in the pairing of homologous chromosomes and formation of SCs by Zip1 polymerization along their axial elements, assisted by the synapsis initiating complex (SIC; Sym et al., 1993; Tsubouchi et al., 2008; Lee et al., 2012). Being the integral SC component that cross-links paired axial elements, Zip1 serves as a marker for synapsis, and its localization pattern is a measure of the extent of SC formation. In the absence of a functional MNC complex, chromosome dynamics are impaired, subsequent events of meiosis become delayed or disrupted, and the fidelity of chromosome segregation is compromised (Chua and Roeder, 1997; Conrad et al., 1997, 2007, 2008; Koszul et al., 2008; Wanat et al., 2008; Sonntag Brown et al., 2011).

We describe the segregation behavior of the multicopy 2 micron plasmid of *S. cerevisiae* during meiosis as a paradigm for the germ-line propagation of selfish extrachromosomal genomes. The 40–60 plasmid copies per haploid cell, and approximately twice as many per diploid cell, reside in the nucleus as mini-chromatin assemblies (Velmurugan et al., 2003; Jayaram et al., 2004b; Ghosh et al., 2006). The nearly chromosome-like stability of the plasmid is conferred by a partitioning system consisting of the plasmid proteins Rep1 and Rep2 and the partitioning locus *STB* (Jayaram et al., 2004a). The Rep–*STB* system ensures equal or nearly equal plasmid segregation by overcoming a diffusion barrier that causes replicated plasmid molecules to be trapped disproportionately in the mother (Murray and Szostak, 1983; Shcheprova et al., 2008; Gehlen et al., 2011; Khmelinskii et al., 2011). The plasmid also houses an amplification system, which rectifies copy number declines resulting from rare missegregation events. A termination-free mode of replication, analogous to rolling circle replication and central to amplification, is thought to be triggered by the inversion of one of the bidirectional forks as a result of a recombination event mediated by the site-specific recombinase Flp (Futcher, 1986; Volkert and Broach, 1986).

The native 2 micron plasmid or a multicopy *STB* reporter plasmid probed by FISH or by operator–fluorescent repressor interaction, respectively, is revealed in mitotic cells as a relatively small number of foci (Velmurugan et al., 2000; Heun et al., 2001). The segregation features of the *STB* reporter plasmid are consistent with each focus, which likely comprises a group of plasmid molecules, being an independent unit of segregation (Liu et al., 2013). Current evidence suggests that the plasmid segregates by physically associating with chromosomes and hitchhiking on them. Furthermore, plasmid sisters formed by the replication of a single-copy 2 micron derivative segregate as if they were tethered to sister chromatids (Ghosh et al., 2007; Liu et al., 2013).

Several chromosome segregation factors are found associated with both *CEN*s and *STB*: the RSC2 chromatin remodeling complex, the Kip1 nuclear motor, the histone H3 variant Cse4 (CENP-A), and the cohesin complex (Mehta et al., 2002; Hajra et al., 2006; Ghosh et al., 2007, 2010; Cui et al., 2009; Huang et al., 2011a; Ma et al., 2013). Pairing of plasmid sisters by cohesin (Ghosh et al., 2007, 2010) would be consistent with their attachment to sister chromatids. However, the highly substoichiometric

association of cohesin and Cse4 with *STB* (Ghosh et al., 2010; Huang et al., 2011b) raises concerns regarding their functional relevance, unless they act in a catalytic manner. Circumstantial evidence suggests that the atypical point *CEN* of budding yeasts and the *STB* locus might share an ancestor that once directed both chromosome and plasmid segregation (Malik and Henikoff, 2009; Huang et al., 2011a; Jayaram et al., 2013). The present day associations of *CEN* binding factors at *STB* may be relics of that shared evolutionary history.

The 2 micron plasmid is propagated efficiently during meiosis as well (Brewer and Fangman, 1980; Hsiao and Carbon, 1981). The presence of double the haploid plasmid content in a diploid cell suggests that, during meiosis, the plasmid undergoes a reductional event that parallels chromosome haploidization. It is not known whether there are common meiosis-specific host factors that interact with *CEN* and *STB*. When the monopolin complex is inappropriately expressed in mitotically dividing cells, it associates with *CEN* but not with *STB* (Liu et al., 2013). In light of the potential ancestral relatedness between *STB* and *CEN*, and between chromosome and 2 micron plasmid segregation pathways, it is possible that a subset of the proteins that regulate *CEN* function and behavior during meiosis may play analogous roles at *STB*.

Intrigued by how plasmid segregation is modulated during meiosis, we characterized the localization and dynamics of a fluorescence-tagged *STB* reporter plasmid during meiotic prophase, followed its segregation during meiosis I, and analyzed its distribution into spores at the end of meiosis II. Our findings are consistent with the potential association of the 2 micron plasmid with *TEL*s by way of the envelope motor responsible for driving chromosome movements that presage homologue pairing. 2 micron plasmid segregation as a *TEL* appendage during meiosis I would signify hitchhiking on chromosomes as the underlying logic that unifies faithful plasmid propagation during both vegetative and germ-line divisions of the host cells.

Results

Segregation of a multicopy *STB* reporter plasmid during meiosis

To characterize plasmid partitioning during meiosis, we used a fluorescence-tagged multicopy *STB* reporter plasmid (Mehta et al., 2002; Cui et al., 2009), with an autonomously replicating sequence (*ARS*) plasmid lacking *STB* as a control (see Materials and methods).

During meiosis I, the *STB* plasmid segregated equally (n:n) or almost equally (n:n − 1) to the two daughter nuclei ∼76% of the time (Fig. 1, A and C). Unequal segregation (n:n′) was seen in ∼23% of meiosis I divisions. Total plasmid missegregation (n:0) was quite low (∼1%). In contrast, the values for the control *ARS* plasmid were ∼29% equal and ∼57% unequal segregation along with ∼14% total missegregation events (Fig. 1, B and C). After meiosis II, asci with all four plasmid-containing spores were ∼68% and ∼22% for the *STB* and *ARS* plasmids, respectively (4:0; Fig. S1, A and B). In the subset of tetrads with no less than four plasmid foci per tetrad, this difference was ∼84% (*STB* plasmid) to ∼48% (*ARS* plasmid; Fig. S1 C).
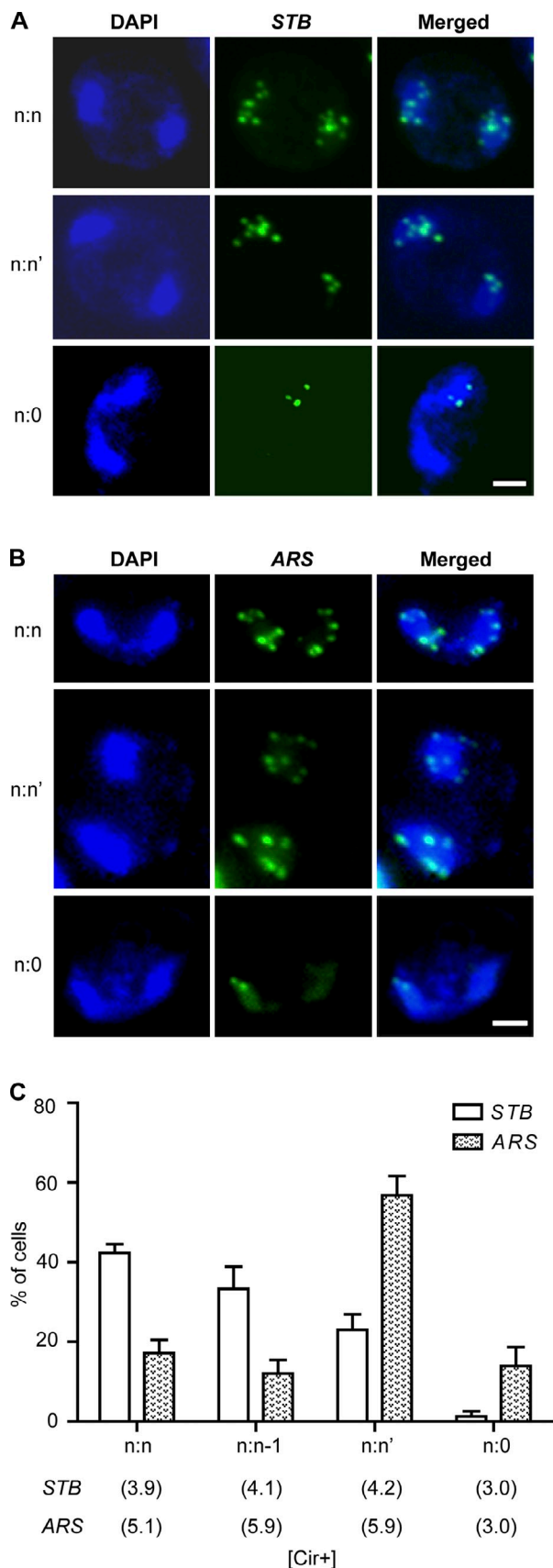
Figure 1. **Plasmid segregation during meiosis I.** (A and B) The segregation of fluorescence-tagged *STB* and *ARS* (lacking a partitioning system) reporter plasmids (Mehta et al., 2002; Cui et al., 2009) was scored in

[cir+] diploid cells by counting plasmid foci in each daughter nucleus at the end of meiosis I. Bars, 2 μm. (C) In the bar graph representation, the n:n and n:n − 1 classes denote equal (or nearly equal) plasmid segregation; the n:n' and n:0 classes denote missegregation and segregation failure, respectively. There is some uncertainty in these numbers as foci occasionally tend to overlap and the number of plasmid molecules in each focus is unknown. The mean number of plasmid foci per nucleus for each segregation class is given below the graphs. These data represent 80 and 90 binucleate cells analyzed for the *STB* and *ARS* plasmids, respectively. The error bars indicate ± SEM.
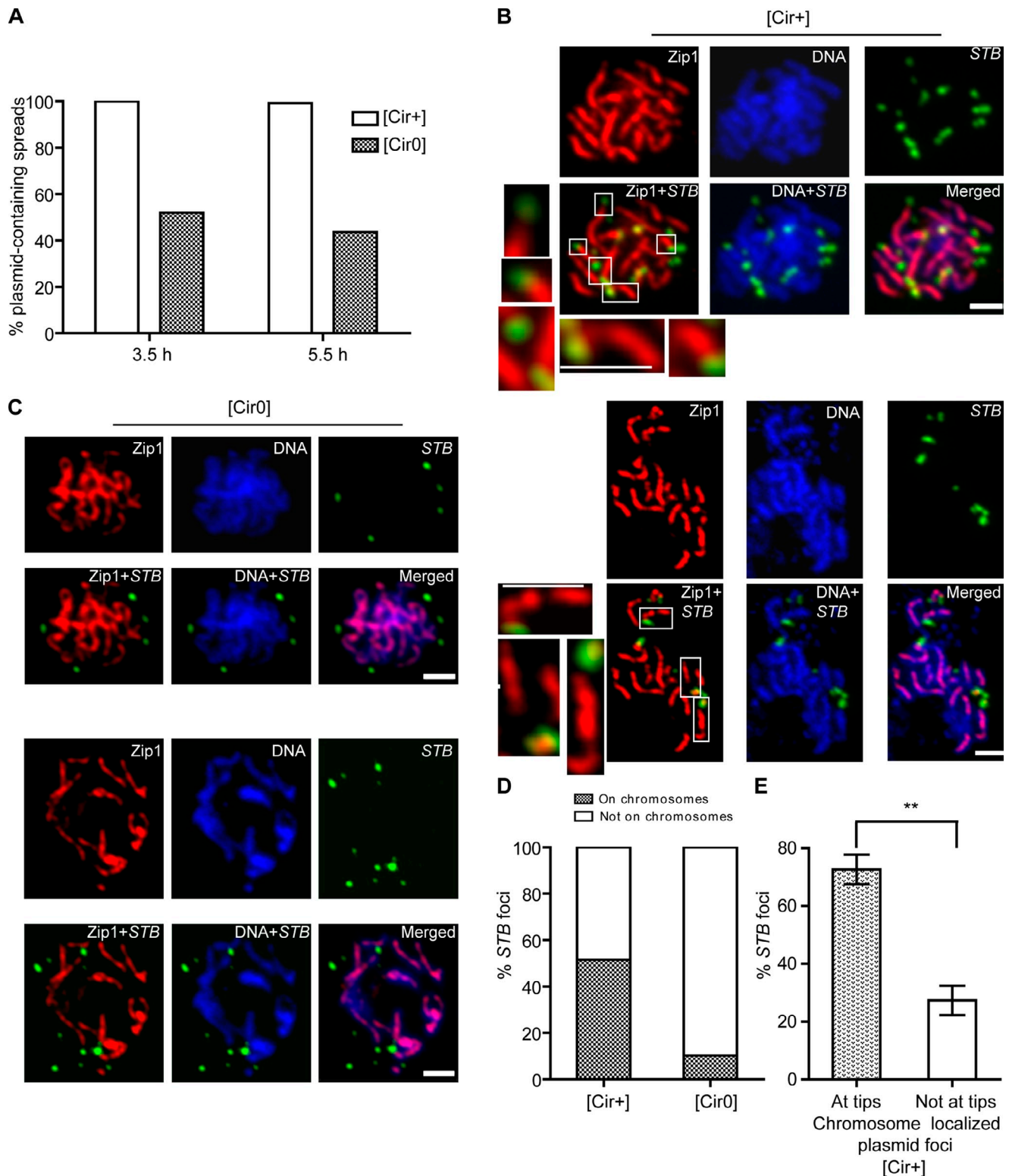
Furthermore, the type I subgroup of the 4:0 class, equal in plasmid foci number in all four spores or in pairs of spores (but not between pairs), was also larger for the *STB* plasmid (~35% vs. ~16%; Fig. S1, D and E).

The distinct equal segregation frequencies for the *STB* and *ARS* plasmids during meiosis I, which are similar to those during mitosis (Velmurugan et al., 2000; Cui et al., 2009), suggest that meiosis I plasmid segregation is driven by the Rep–*STB* system. Because sister spores are not ordered in the ascus, the assessment of equal segregation during meiosis II is not straightforward. Nevertheless, the difference between the *STB* and *ARS* plasmids in the representation of type I tetrads (Fig. S1 E; $P < 0.05$) suggests that the 2 micron plasmid partitioning system is active during meiosis II as well.

Localization of *STB* plasmids in meiotic chromosome spreads

To examine whether *STB* plasmids are associated with chromosomes, as expected from the hitchhiking model, we screened surface spread nuclei (chromosome spreads) from cells at the early (leptotene/zygotene) and late (pachytene) stages of meiosis I. The *STB* plasmid was found in all chromosome spreads from [cir+] cells, whereas roughly half the spreads from [cir0] cells (lacking the Rep proteins) contained no detectable plasmid (Fig. 2 A). As there was higher plasmid loss in the [cir0] strain compared with the [cir+] strain during the mitotic divisions preceding meiosis, the fraction of plasmid-containing cells in the spread assays was smaller for the [cir0] strain. The data corrected for this difference (Fig. 2 A) suggest potential tethering of *STB* plasmids to chromosomes in a Rep1-Rep2–dependent manner. There is a caveat that the spreads may include, in addition to chromosomes, nuclear membrane fragments and nuclear matrix–associated proteins.

Next, we mapped plasmid foci in pachytene spreads (containing better resolved chromosomes) from [cir+] (Fig. 2 B) and [cir0] (Fig. 2 C) strains with respect to DAPI using the criteria described in the Materials and methods section. A considerable fraction of the *STB* plasmid foci (~52%) was associated with chromosomes, <0.4 μm away, in the [cir+] host (Fig. 2, B and D). Within this subpopulation, ~73% was at chromosome tips, which suggests preferential plasmid association with *TEL*s (Fig. 2 E). Plasmid–chromosome association required Rep1 and Rep2 proteins, as indicated by the [cir0] strain (Fig. 2, C and D). The results were similar when Zip1, which marks the axis of paired homologues (Sym et al., 1993), served as the chromosome reference (unpublished data).

Figure 2. **Localization of the *STB* reporter plasmid in meiotic chromosome spreads.** (A) Chromosome spreads were prepared from isogenic [cir+] or [cir0] cells (transformed by the *STB* reporter plasmid) at the leptotene/zygotene or the pachytene stage of meiosis I (3.5 h and 5.5 h after transfer to sporulation medium, respectively). The results were corrected for differences in the percentages of [cir+] and [cir0] cells harboring the reporter plasmid at the time of transfer to sporulation medium. The histograms represent data from ~200 spreads for t = 3.5 h and ~800 spreads for t = 5.5 h. In these and subsequent spread assays, the plasmid was detected using an antibody to GFP, which targets the GFP-LacI bound to the LacO array present on the plasmid. (B and C) In the pachytene spreads, chromosomes were visualized by DAPI and the central axes of paired chromosomes by Zip1 (using an antibody to the native protein). Selected sections (boxed regions) of the spreads are enlarged 3× to highlight plasmid foci at chromosome tips. Bars, 2 µm. (D) For the plasmid foci analyzed (>150 for [cir+] spreads; >100 for [cir0] spreads), a plasmid-to-chromosome separation of <0.4 µm was interpreted as colocalization of the two. (E) The chromosome-associated plasmid foci from the [cir+] spreads were distinguished into those at chromosome tips or away from them. The error bars indicate ± SEM. **, P < 0.01 (two-tailed *t* test).

The chromosome spread patterns would be consistent with the association of the *STB* plasmid with *TEL*s or with the nuclear periphery at or near sites for *TEL* anchoring. Membrane-associated *TEL*s (Zickler and Kleckner, 1998; Scherthan, 2007) are responsible for propagating RPMs generated by envelope motor assemblies along chromosome arms (Scherthan et al., 2007; Conrad et al., 2008; Koszul et al., 2008). Plasmid foci detected outside chromosomes might indicate the dynamic nature of plasmid–chromosome association. Alternatively, they might denote plasmids associated with segments of the nuclear membrane that were detached from *TEL*s.

Localization of *STB* plasmids with respect to Ctf19, Mps3, and Rap1

The suggested localization of *STB* plasmids at or proximal to *TEL*s (Fig. 2, B, D, and E) was further verified against Ctf19 and Mps3 as *CEN* and *TEL* markers, respectively. Ctf19, an outer kinetochore protein, is a member of the COMA subcomplex (Hyland et al., 1999; Westermann et al., 2007). Mps3, a SUN domain nuclear envelope protein, is a component of the spindle pole body in mitotic and meiotic cells, and becomes associated with *TEL*s during meiotic prophase (Conrad et al., 2007). Plasmid locations were further verified with respect to the *TEL* marker Rap1 (Klein et al., 1992).

Association of the *STB* plasmid with Mps3 and Rap1 (∼53% and ∼46%, respectively, at leptotene/zygotene; ∼77% and ∼71%, respectively, at pachytene) was conspicuously higher than that with Ctf19 (∼14% at leptotene/zygotene and ∼8% at pachytene; Fig. 3, A–H). In spreads prepared from cells immediately after transfer to sporulation medium, the fractions of plasmid foci colocalized with Ctf19 (∼11%) and Rap1 (∼41%) were not different from those at leptotene/zygotene (unpublished data). Thus, approximately half of the *STB* plasmid population resides at or near *TEL*s during early meiosis, with a significant increase in this population at late stages of meiosis I (70–80%). *CEN* proximal localization of the plasmid during meiosis is quite rare.

Association of Rep1 with chromosomes

Rep1 and Rep2 associate with each other and localize to mitotic chromosome spreads in a mutually dependent manner (Velmurugan et al., 2000; Mehta et al., 2002). Consistent with their in vivo interaction with *STB* (Velmurugan et al., 1998), an *STB* reporter plasmid is recruited to the spreads with the assistance of both proteins. To test whether a similar mechanism operates in meiosis, the presence of Rep1 in meiotic chromosome spreads, as well as plasmid localization with respect to Rep1, was examined.

Rep1 formed a distribution of foci in pachytene chromosome spreads (Fig. 4 A), the majority (∼75%) being larger and more intense than the rest. The *STB* reporter plasmid foci, fewer in number than the Rep1 foci, were almost always coincident with a subset of the latter (Fig. 4 A). Among the ∼60% Rep1 foci that were localized on, or abutted, DAPI-stained chromosomes (<0.4 µm separation; Fig. 4 B and C), the vast majority (∼70%) were present at chromosome tips (Fig. 4 C). This preferential localization was further ascertained with respect to Zip1 (Fig. 4 B).

The 2 micron plasmid appears to be delivered to its nuclear address during meiosis by the Rep proteins, presumably via their interaction with a *TEL*-associated protein or a membrane protein that associates with *TEL*s.

RPMs of the *STB* reporter plasmid

The rapid *TEL*-led chromosome movements during meiotic prophase (Scherthan, 2006; Scherthan et al., 2007; Conrad et al., 2008; Koszul et al., 2008; Wanat et al., 2008) can be quantitatively described by their (a) mean speed, (b) maximum speed, and (c) bias (Conrad et al., 2008; Lee et al., 2012). Bias is a measure of chromosome displacement, with values of 0, <0, and >0 denoting random motion, the tendency to stay in place, and the tendency to travel far, respectively. The speeds decrease in the order *TEL* > mid-chromosomal locus > *CEN*. Furthermore, paired *TEL*s display higher mean and maximum speeds as well as larger bias than unpaired *TEL*s (Conrad et al., 2008; Fig. 5). If the 2 micron plasmid is tethered to chromosomes, the plasmid movements should mimic chromosome movements, and also disclose the chromosomal locus that it is associated with. We characterized the prophase movements of the *STB* reporter plasmid with respect to either native *TEL*s or an 81-bp stretch of the *TEL* repeat ($G_{1-3}T$) units located in a *CEN*-based circular plasmid.

The maximum speed, mean speed, and bias distributions of the *STB* plasmid in the wild-type background were nearly identical to those of unpaired *TEL*s or of the *CEN-ARS-TEL* plasmid (Fig. 5, A–C; and Videos 1 and 2), but differed from those of paired *TEL*s (Fig. 5, D–F). In contrast, a *CEN-ARS* plasmid had clearly reduced values for all three parameters (Fig. 5, G–I), as expected for a lack of motor-driven mobility. However, a small fraction of the plasmids did match paired *TEL*s in the distances traversed (bias values of 0.1–0.4; Fig. 5 I). The movements of a multicopy *ARS* plasmid were also quite different from those of the *STB* plasmid, the *CEN-ARS-TEL* plasmid, and unpaired or paired *TEL*s (unpublished data).

The dynamics data suggest that an *STB*- or *TEL*-containing plasmid engages the meiotic RPM machinery, leading to their nearly identical patterns of movement. They are consistent with the *STB* plasmid gaining access to the envelope motor first and then associating with unpaired *TEL*s, or vice versa. The resemblance of the *STB* plasmid to unpaired and not paired *TEL*s may be a matter of timing. These measurements were done at a stage when most *TEL*s were still unpaired. Indeed, colocalization of *STB* plasmid foci with telomeric marker proteins in pachytene stage chromosome spreads (Fig. 3, E and G, bottom) would suggest that the plasmid can associate with paired *TEL*s. The contrasting prophase dynamics of the *STB* and *ARS* plasmids attest to the crucial role of the 2 micron plasmid partitioning system in promoting *TEL*-like plasmid movement.

The roles of bouquet-RPM proteins in the prophase dynamics of the *STB* plasmid

As alluded to earlier, the MNC complex functions in meiosis by promoting the bouquet formation–RPM pathway (Trelles-Sticken et al., 2005; Scherthan et al., 2007; Conrad et al., 2008; Koszul et al., 2008; Wanat et al., 2008; Lee et al., 2012). All three contribute toward timely pairing of homologues, normal
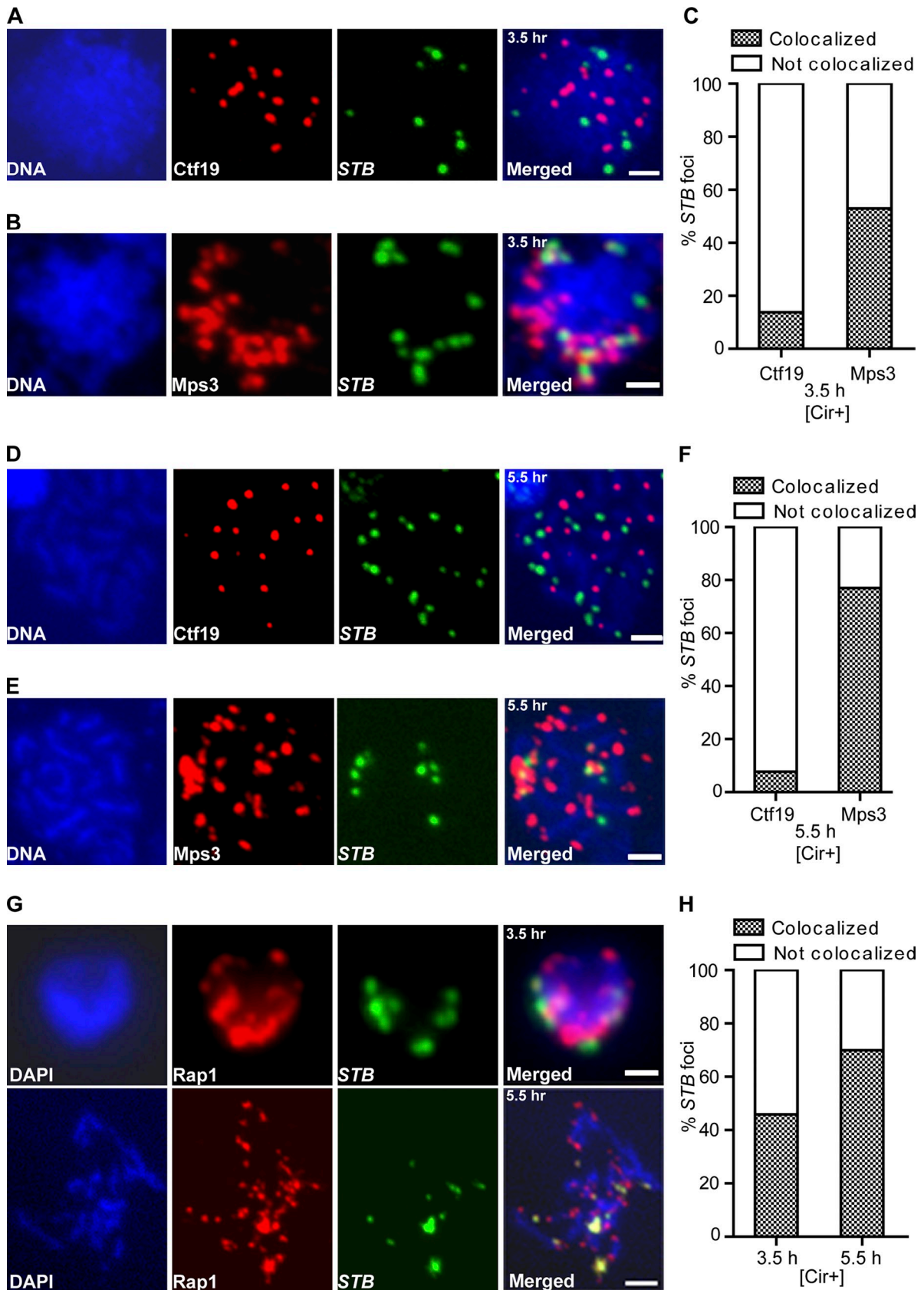
Figure 3. **Localization of the *STB* reporter plasmid with respect to *CEN*- and *TEL*-specific marker proteins.** Chromosome spreads were prepared at 3.5 h (leptotene/zygotene) and 5.5 h (pachytene) into meiosis. Plasmid foci were mapped with Ctf19 (A, C, and D) as the *CEN* marker and Mps3 (B, E, and F) or Rap1 (G and H) as the *TEL* marker. The antibodies for visualizing Ctf19 (*CTF19-MYC*), Mps3 (*MPS3-HA*), and Rap1 (*RAP1-RFP*) were anti-Myc, anti-HA, and anti-RFP, respectively. In each localization assay, ~150 plasmid foci were scored. Bars, 2 µm.
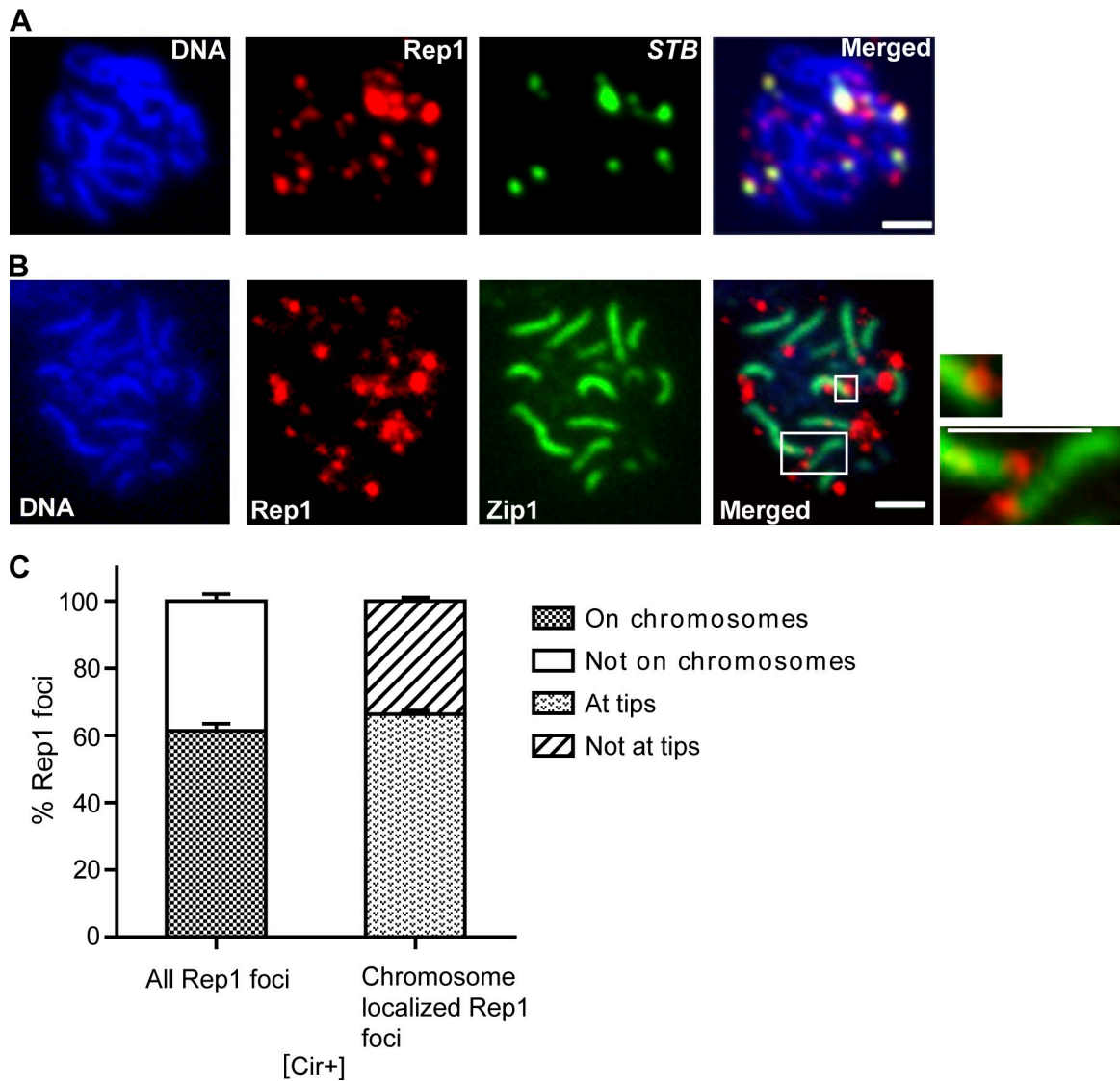
Figure 4. **Localization of Rep1 with respect to the *STB* reporter plasmid and Zip1.** (A) In chromosome spreads prepared from pachytene cells (5.5 h in sporulation medium), Rep1 was visualized along with the *STB* reporter plasmid. (B) Rep1 foci were detected using an antibody to the native protein, with Zip1 as the chromosome marker. Bars, 2 µm. (C) The histogram at the left represents the fraction of Rep1 foci (from a total of >125 analyzed) that were localized on chromosomes (<0.4 µm separation). Within this subset, the fraction present at chromosome tips (the boxed regions, shown in 3× enlarged views on the right, depict examples of such Rep1 foci) was plotted in the histograms at the right. The error bars indicate ± SEM.

meiotic recombination, and curtailment of ectopic or nonallelic recombination and aneuploidy (Chua and Roeder, 1997; Conrad et al., 1997, 2007; Trelles-Sticken et al., 2000; Kosaka et al., 2008; Wanat et al., 2008). Whereas Mps3 and Ndj1 collaborate to anchor *TEL*s at the nuclear envelope, Csm4 is essential for their bouquet organization, and is likely the force transducer. We used *ndj1Δ* and *csm4Δ* to test the pertinence of *TEL*–membrane association, bouquet formation, or force generation to prophase movements of the *STB* plasmid.

In the absence of Csm4, analogous to chromosomes, the *STB* plasmid foci were slowed down considerably and displayed a smaller bias (Fig. 6, A–C; and Videos 1 and 2). The decrease in maximum and average speeds was more pronounced at 7 h than at 4 h (Fig. 6, A and B). At 4 h, the *STB* plasmid average and maximum speeds exceeded those of unpaired and paired *TEL*s but resembled those of the *CEN-ARS-TEL* plasmid (Fig. S2,

A, B, D, and E). At this time point, the *STB* plasmid closely matched unpaired *TEL*s and the *CEN-ARS-TEL* plasmid in bias, and only modestly differed from paired *TEL*s (Fig. S2, C and F). At 7 h (for the plasmids) and 8 h (for the chromosomes; Fig. 6, D–F and G–I), the *STB* plasmid was most similar to paired *TEL*s in average speeds and to the *CEN-ARS-TEL* plasmid in maximum speeds and bias. The *STB* plasmid maximum speeds were intermediate between those of unpaired and paired *TEL*s. The points to note are the marked reduction in *STB* plasmid speeds as meiosis I progressed in the *csm4Δ* strain, and the manifestation in *STB* plasmid dynamics of mixed features of unpaired and paired *TEL*s and of the *CEN-ARS-TEL* plasmid.

The lack of Ndj1, which reduces prophase movements of *TEL*s less markedly than *csm4Δ* (Conrad et al., 2008), also altered *STB* plasmid dynamics in a similar manner (Videos 3 and 4). In a reversal of the trend in the *csm4Δ* strain, the decreased
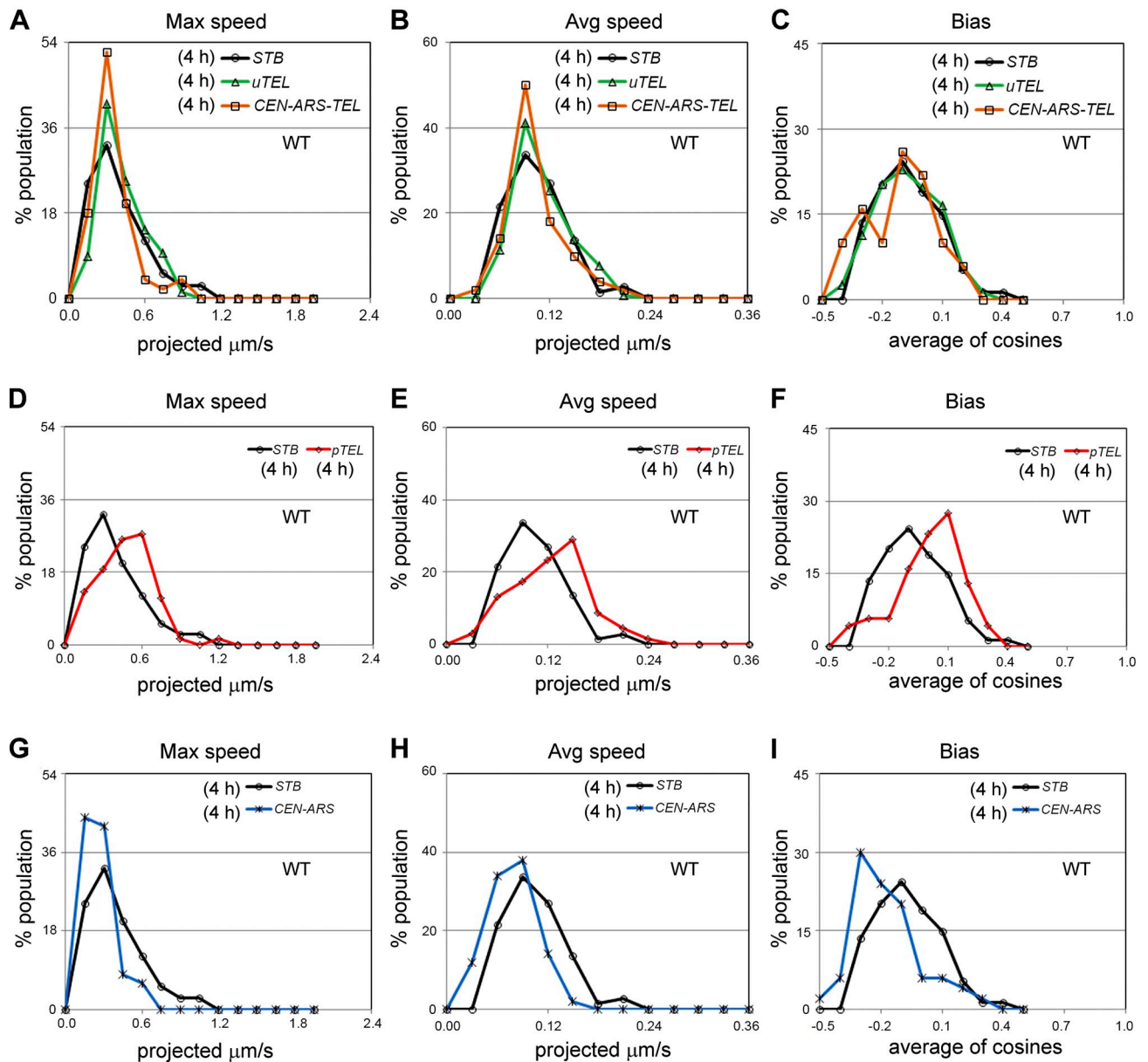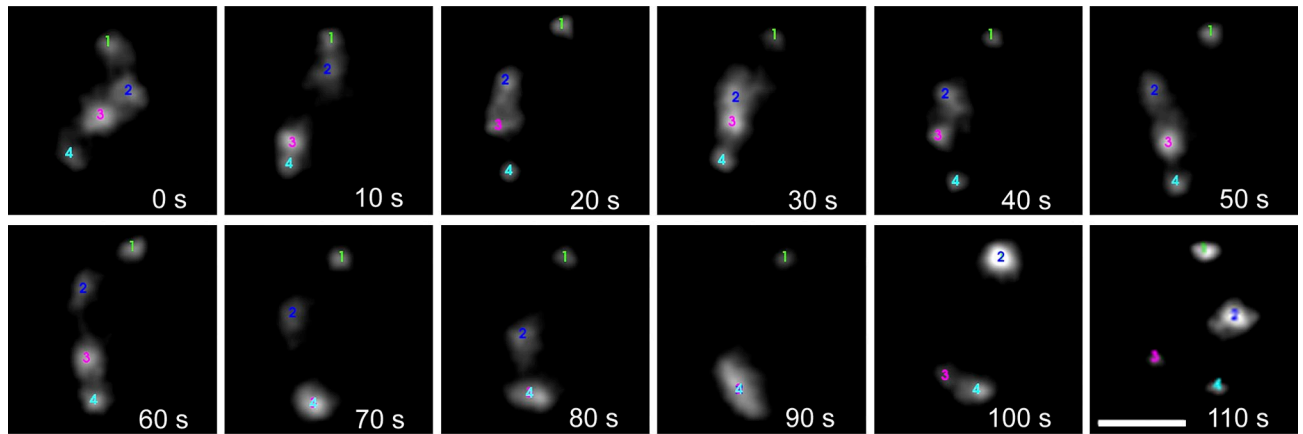
Figure 5. **Characterization of *STB* plasmid movements during prophase.** In this through-focus time-lapse analysis of wild-type cells (Conrad et al., 2008), at least 35 plasmid foci (tagged by green fluorescence) were traced over a period of 2 min at 1 frame/2 s. The relative positions of four individual plasmid foci (marked 1–4) in a single nucleus at 10-s intervals are displayed at the top. Bars, 2 µm. Chromosome *VIIL TEL*s tagged by red fluorescence were also
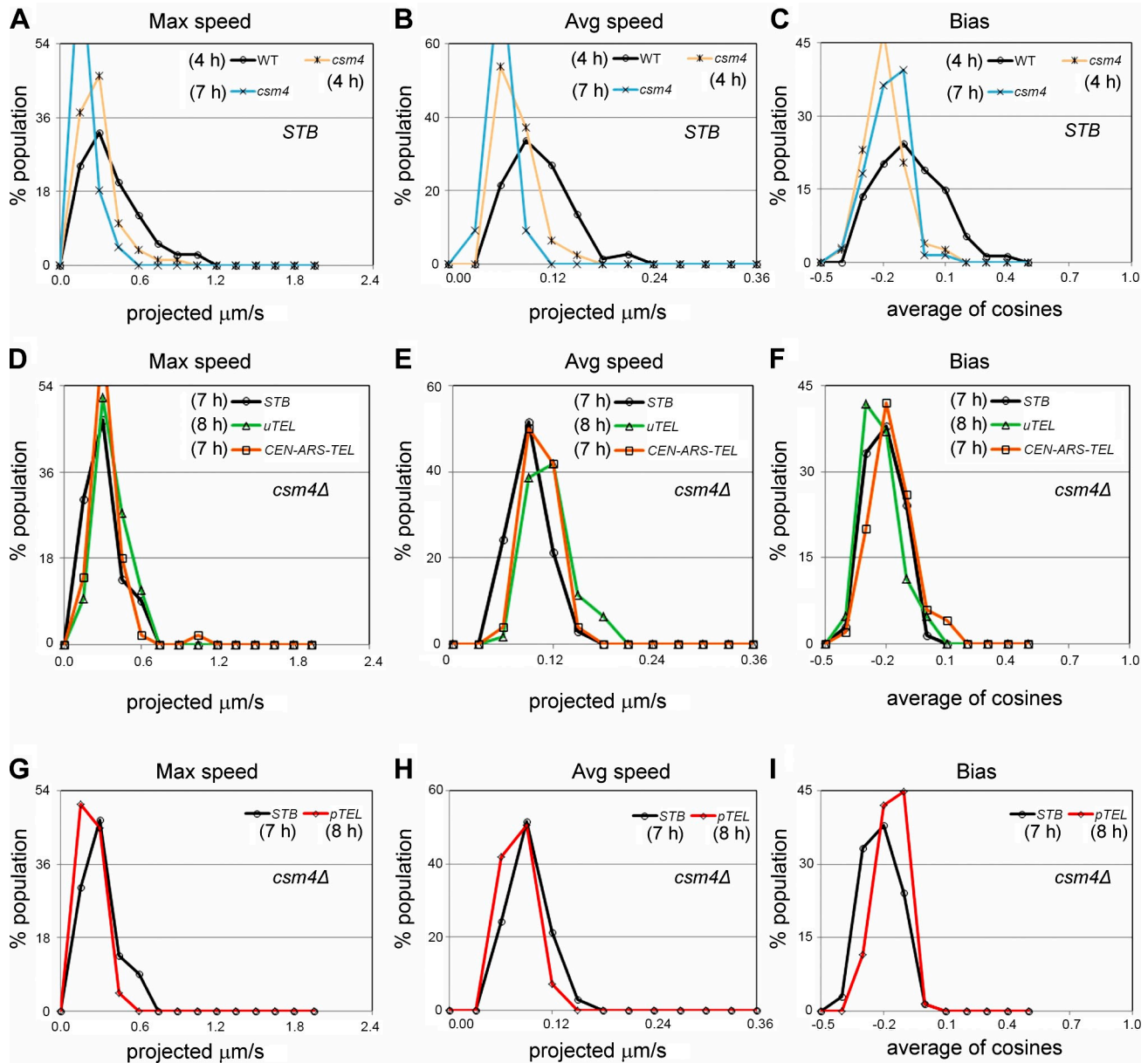
Figure 6. Dynamics of the *STB* reporter plasmid in the absence of Csm4. The mobility features of the *STB* plasmid in the wild-type (4 h after transfer of cells to sporulation medium) and *csm4Δ* (4 h and 7 h after transfer) strains were plotted side by side (A–C). These graphs were based on 1 frame/2 s time-lapse data. As *csm4Δ* delays the meiotic program, the 4 and 7 h time points correspond to comparable prophase stages of meiosis I between the wild-type and the mutant strains, respectively. Plots comparing the *STB* plasmid to the plasmid-borne *TEL* (D–F, *CEN-ARS-TEL*) or chromosome *IVR TELs* (D–F, unpaired = u*TEL*; G–I, paired = p*TEL*) were assembled from data obtained at 1 frame/s. The analyses for the plasmids and for chromosomal *TELs* were done at 7 h and 8 h, respectively, after initiation of meiosis. This time difference did not alter the dynamics of paired or unpaired *TELs* (unpublished data). Note that a difference in time resolution in plotting the same set of recorded movements, 1 frame/2 s versus 1 frame/1 s, changes the histogram shapes; e.g., the plots for the *STB* plasmid in the *csm4Δ* mutant at 7 h in A and D (see the Materials and methods).

STB plasmid speeds at 4 h due to *ndj1Δ* were ameliorated at 7 h, with a similar effect on the bias as well (Fig. S3, A–C). The *STB* plasmid was similar to paired *TELs* at 4 and 7 h (Fig. S2, J–L; and Fig. S3, G–I) and, except for modest differences in bias, to the *CEN-ARS-TEL* plasmid at 4 h (Fig. S2, G–I). At 4 h,

the *STB* plasmid was also similar to unpaired *TELs* in maximum speeds and bias but differed in average speeds (Fig. S2, G–I). At 7 h, the *STB* plasmid maximum speeds and bias exceeded those of unpaired *TELs* and the *CEN-ARS-TEL* plasmid, whereas all three were similar in average speeds (Fig. S3, D–F). The higher

traced over the 2-min period (1 frame/2 s) as an internal standard (shown in Fig. S3). The speeds and bias of the *STB* plasmid were plotted alongside those for a *CEN*-based plasmid harboring the *TEL* repeat (*CEN-ARS-TEL*; A–C), the chromosome *IVR TELs* in the unpaired (u*TEL*; A–C) and paired (p*TEL*; D–F) states, and for a *CEN*-based *ARS* plasmid (*CEN-ARS*; G–I). The values for chromosome dynamics used in these plots and those in Fig. 6 and Fig. S3 were taken from previously published results (Conrad et al., 2008).
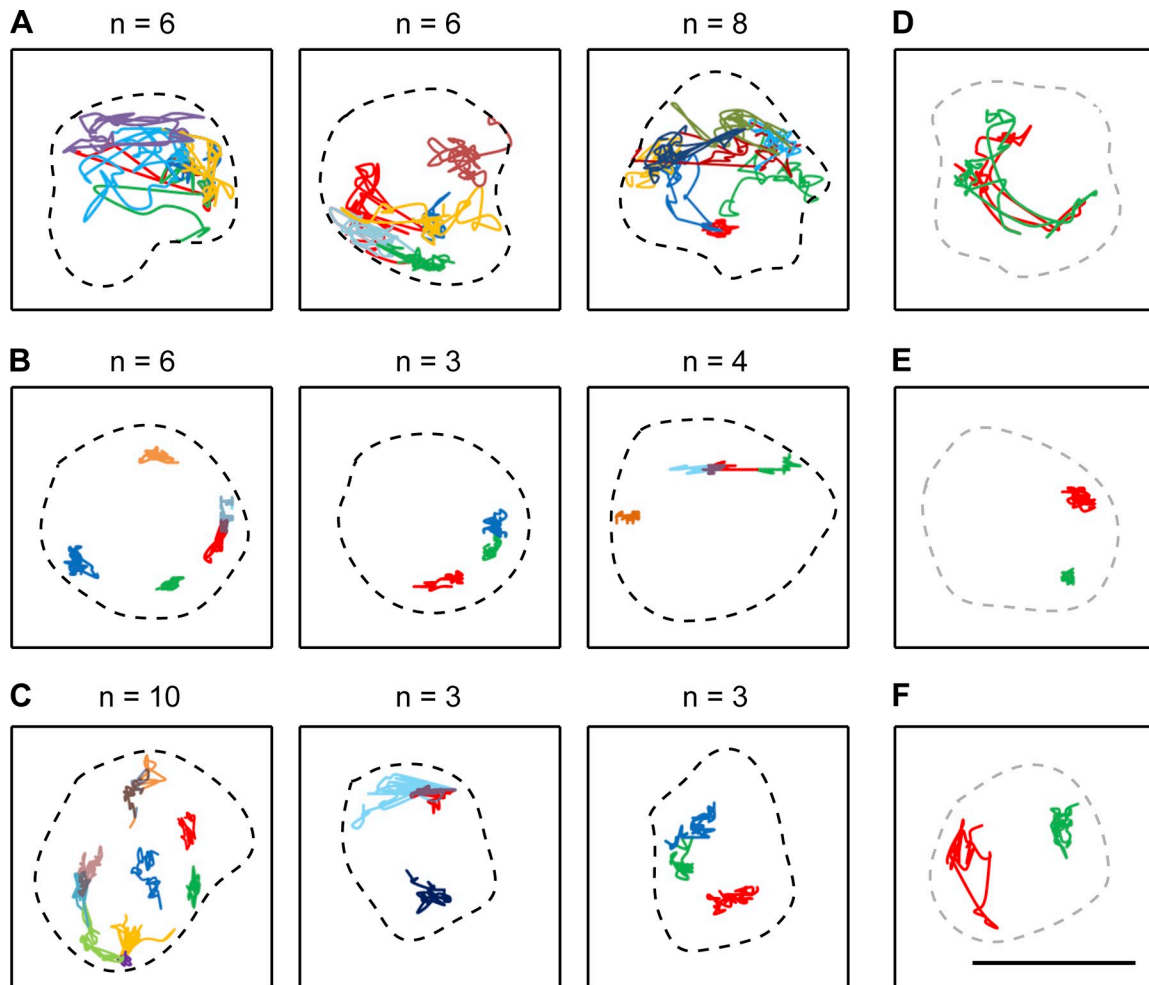
Figure 7. **Movement of individual *STB* plasmid foci in wild-type, *csm4Δ*, and *ndj1Δ* strains.** The traces from three representative cells each illustrate the excursions of individual plasmid foci (denoted by different colors) over a 1-min period in the wild-type (A), *csm4Δ* (B), and *ndj1Δ* (C) strains (Fig. 5, Fig. 6, and Fig. S3; and Videos 2 and 4). The plasmid foci were visualized at 4 h (wild type) and at 7 h (mutants) after transfer to sporulation medium. The nuclear periphery (broken lines) is an approximate representation deduced from a single frame of each 60-frame movie, based on background nuclear fluorescence from GFP-LacI. For comparison, the paths traversed by unpaired *IVR TELs* over a 1-min span are depicted in D–F (Videos 1 and 3). As the pertinent nuclei images were not available, the nuclear outlines in D–F were arbitrarily chosen from the plasmid movies representing the relevant genetic backgrounds. *n* = number of plasmid foci in a nucleus. Bar, 2 µm.

speed shoulder in the maximum speed plot for the *STB* plasmid at 7 h was absent at 4 h.

Except for some decrease in the maximum speeds in the *csm4Δ* mutant, the *CEN-ARS* plasmid was largely indifferent to the absence of Csm4 or Ndj1 (Fig. S4, A–I), and showed no significant time-dependent changes in its dynamics. Individual time traces highlight not only the *TEL*-like dynamics of the *STB* plasmid but also the similarity in their slowdown by *csm4Δ* or *ndj1Δ* (Fig. 7). This striking resemblance between them is most easily explained by the same motor and force transducer being responsible for their prophase dynamics.

The similarity of the *STB* and *CEN-ARS-TEL* plasmids to each other and to unpaired *TELs* in the wild-type host (at 4 h) suggest that these plasmids engage the RPM machinery similarly to, or hitchhike on, unpaired *TELs* during early prophase. The changes in the *STB* plasmid speeds in the *csm4Δ* and *ndj1Δ* strains at 4 h versus 7 h and the shoulder in the maximum plasmid speed histograms at 7 h, prominent in the *ndj1Δ* strain (Fig. S3, D and G) and less so in the *csm4Δ* strain (Fig. 6, D and G), would be

consistent with the plasmid accessing the motor unassisted by chromosomes. However, plasmid mobility may be modulated by the association of *TELs* with the motor and potential plasmid–*TEL* tethering.

It is not clear why the features of *STB* plasmid dynamics in the mutants are split among those of unpaired and paired *TELs* and the *CEN-ARS-TEL* plasmid, and why these similarities or differences change with time. Possible reasons are differences between plasmid and chromosome loads on the motor, interactions of the plasmid with unpaired versus paired *TELs*, and changes in the relative fractions of these two *TEL* classes as a function of the stage of meiosis. The *CEN-ARS-TEL* plasmid also displays split features of unpaired and paired *TELs*. If this plasmid were autonomous in its mobility, it is expected to behave like unpaired *TELs*. The complexity inherent in chromosome movements would be reflected in the movements of chromosome-associated plasmids as well. A chromosome at the leading edge of motion shows more dramatic translations than the "follower" chromosomes (Koszul et al., 2008). Leadership changes

among chromosomes, and an occasional "maverick" leader displays particularly prominent displacements (Scherthan et al., 2007; Koszul et al., 2008). A leader may in certain instances lose its followers, thus becoming an isolated "orphan" chromosome. Because of these potential complicating factors, strict quantitative adherence of the *STB* plasmid to paired or unpaired *TEL*s in its movements would be unlikely.

Localization of *STB* plasmid foci in *ndj1Δ* and *csm4Δ* mutants

The results thus far suggest that the *STB* plasmid interacts with sites at the nuclear periphery where *TEL*s localize, or with *TEL*s themselves. Anchoring of *TEL*s to the nuclear envelope is stabilized by Ndj1 but does not require Csm4, which promotes clustering of *TEL*s and their coupling to the force generator (Trelles-Sticken et al., 2000; Conrad et al., 2007, 2008; Kosaka et al., 2008). If association occurs primarily between membrane-localized plasmids and *TEL*s, *ndj1Δ* is expected to be more disruptive of this association than *csm4Δ*. We have tested this prediction by measuring plasmid distances from the nuclear periphery in the mutants and by following the effects of *ndj1Δ* on plasmid colocalization with Rap1.

The majority of plasmid foci in pachytene nuclei from the wild-type and *csm4Δ* cells was associated with the outer edge of the DAPI zone, or was internal to it (Fig. 8, A and B). In contrast, in nuclei from *ndj1Δ* cells, several plasmid foci were separated from the DAPI edge, the majority being external to it (Fig. 8, A and B). Among the external foci, those farthest from the DAPI edge were higher in number in the *ndj1Δ* strain than in the wild-type and *csm4Δ* strains (Fig. 8 C). As the DAPI boundary was assigned conservatively, the circumference of the DAPI zone was likely contracted significantly in this analysis. To circumvent this potential complication, foci distances measured from Nup49-labeled nuclear membrane (Fig. 8 D) were converted to plasmid occupancy of nuclear zones 1–3, demarcating cross sections of equal areas (Meister et al., 2010; Materials and methods). The majority of plasmids were situated within the outermost zone (zone 1) in the wild type and in the mutant strains (Fig. 8 E).

Finally, the fraction of plasmid foci colocalizing with Rap1 in pachytene chromosome spreads was not reduced by *ndj1Δ* (Fig. 9, A and B). The average number of Rap1 foci in the deletion strain was ∼45 compared with ∼30 in the wild type (unpublished data), which is consistent with the disruption of the native organization of Rap1 or of its association with *TEL*s (Conrad et al., 1997). The fraction of plasmid foci coincident with chromosomes (<0.4 µm) was reduced to 36% from 52% estimated for the wild type (Fig. 9 C; P < 0.05). Within this subset, the foci associated with chromosome tips were only 47%, a significant reduction from 73% when Ndj1 was functional (Fig. 9 D; P < 0.05).

The *STB* plasmid profiles in the mutant strains indicate that peripheral plasmid localization is unaffected by *ndj1Δ* or *csm4Δ*. The differences in plasmid location with respect to the DAPI boundary versus the nuclear envelope in the *ndj1Δ* strain can be explained by this mutation disrupting the preferential perinuclear chromosome organization seen in the wild-type and

csm4Δ backgrounds (Trelles-Sticken et al., 2000; Conrad et al., 2008; Wanat et al., 2008). In the absence of Ndj1, *TEL*s dissociate from the nuclear membrane, and Rap1 foci tend to be more internalized (Trelles-Sticken et al., 2000). However, the reduction in peripheral Rap1 foci in the mutant is modest (from 52% to 40%). At the same time, their total number increases from ∼30 to between 45 and 60 (Conrad et al., 1997; this study), which indicates extra-telomeric Rap1. As there are far fewer plasmid foci compared with Rap1 foci, the ratio between the two in zone 1 would still favor Rap1. Thus, authentic plasmid colocalization with a subset of Rap1 foci in zone 1 is still possible. The integrity of *TEL*s could be compromised by *ndj1Δ*, affecting *TEL* clustering and perhaps increasing the propensity for frayed chromosome ends. As a result, at least some of the plasmid foci associated with Rap1 may appear to be dislocated from the ends of DAPI-stained chromosomes. Considered in toto, these results suggest that the plasmid establishes a bipartite association with the nuclear membrane and with membrane-anchored *TEL*s, with Rap1 perhaps being responsible for the latter directly or indirectly.

2 micron plasmid segregation in *ndj1Δ* and *csm4Δ* strains

The shared meiotic defects characterized for *ndj1Δ* and *csm4Δ* are consistent with the requirement of Ndj1 and Csm4 in promoting (a) partner interactions during the early phase of recombination; (b) formation, maturation, and resolution of recombination intermediates; and (c) disjunction of homologues during anaphase I (Chua and Roeder, 1997; Conrad et al., 1997; Trelles-Sticken et al., 2000; Kosaka et al., 2008; Wanat et al., 2008). Provided that 2 micron plasmid segregation during meiosis is physically coupled to chromosome segregation, *ndj1Δ* and *csm4Δ* are expected to lower the fidelity of meiotic plasmid segregation. We therefore scored *STB* plasmid segregation in the deletion strains during meiosis I and at completion of meiosis II.

The *STB* plasmid showed higher incidence of missegregation as well as higher segregation failure (n:0) during meiosis I in the absence of Ndj1 or Csm4 (Fig. 10 A). Similarly, there was a reduction in the fraction of asci in which all four spores contained plasmid (Fig. S5 A). An increase in chromosome missegregation in the *ndj1Δ* and *csm4Δ* mutants was also noted (Fig. S5, B and C), as had been previously described (Chua and Roeder, 1997; Conrad et al., 1997; Marston et al., 2004; Wanat et al., 2008).

Thus, disabling components of the envelope motor that promote chromosome dynamics and segregation diminishes the fidelity of meiotic segregation of the 2 micron plasmid.

Discussion

The molecular mechanisms for the nearly chromosome-like stability of the 2 micron plasmid have not been fully elucidated. Equal plasmid segregation during mitosis (Scott-Drew and Murray, 1998; Velmurugan et al., 2000) is unlikely to be mediated by direct microtubule attachment and spindle force or association with the spindle pole body, or with a nuclear membrane protein that is not impeded by a diffusion barrier.
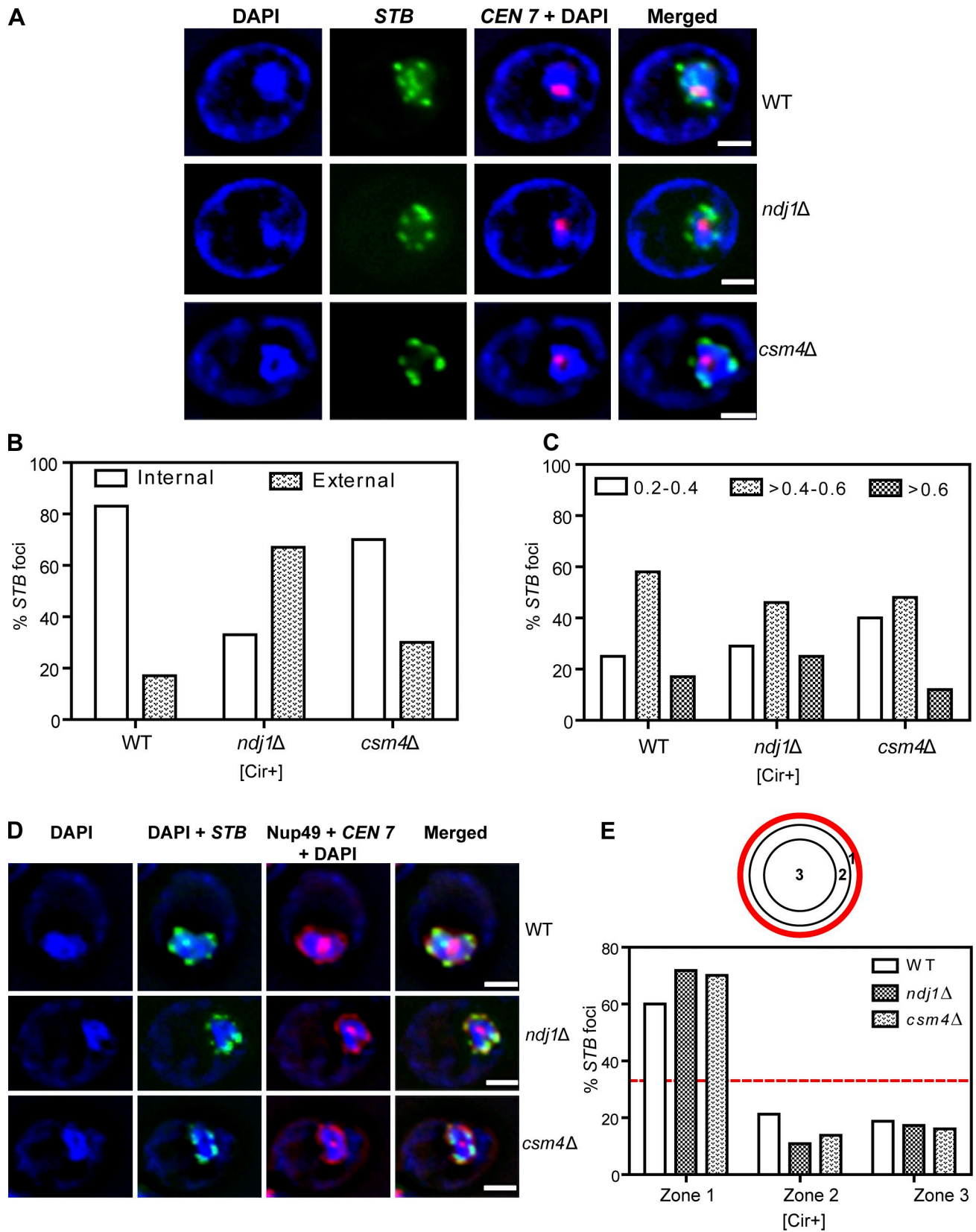
Figure 8. ***STB* plasmid localization at pachytene with respect to nuclear periphery in *ndj1Δ* and *csm4Δ* strains.** (A and B) The nearest distances of individual plasmid foci from the edge of the DAPI staining zone were measured to separate the foci into two groups: "internal" (at the edge of the DAPI zone or within it) and "external" (outside the DAPI boundary). (C) The external group of foci was subdivided into three types, based on the extent of their separation from the boundary. (D and E) Plasmid distances were measured from the nuclear envelope (outlined by Nup49-mCherry) along the diameter of circular cross sections of the nucleus (Meister et al., 2010). They were distributed into three zones (1–3) of equal area by placing the zone 1–2 boundary at $\sqrt{(2/3 \times R)}$ and the zone 2–3 boundary at $\sqrt{(1/3 \times R)}$, where R = the radius of the circle. The dashed line in E marks the probability of the random
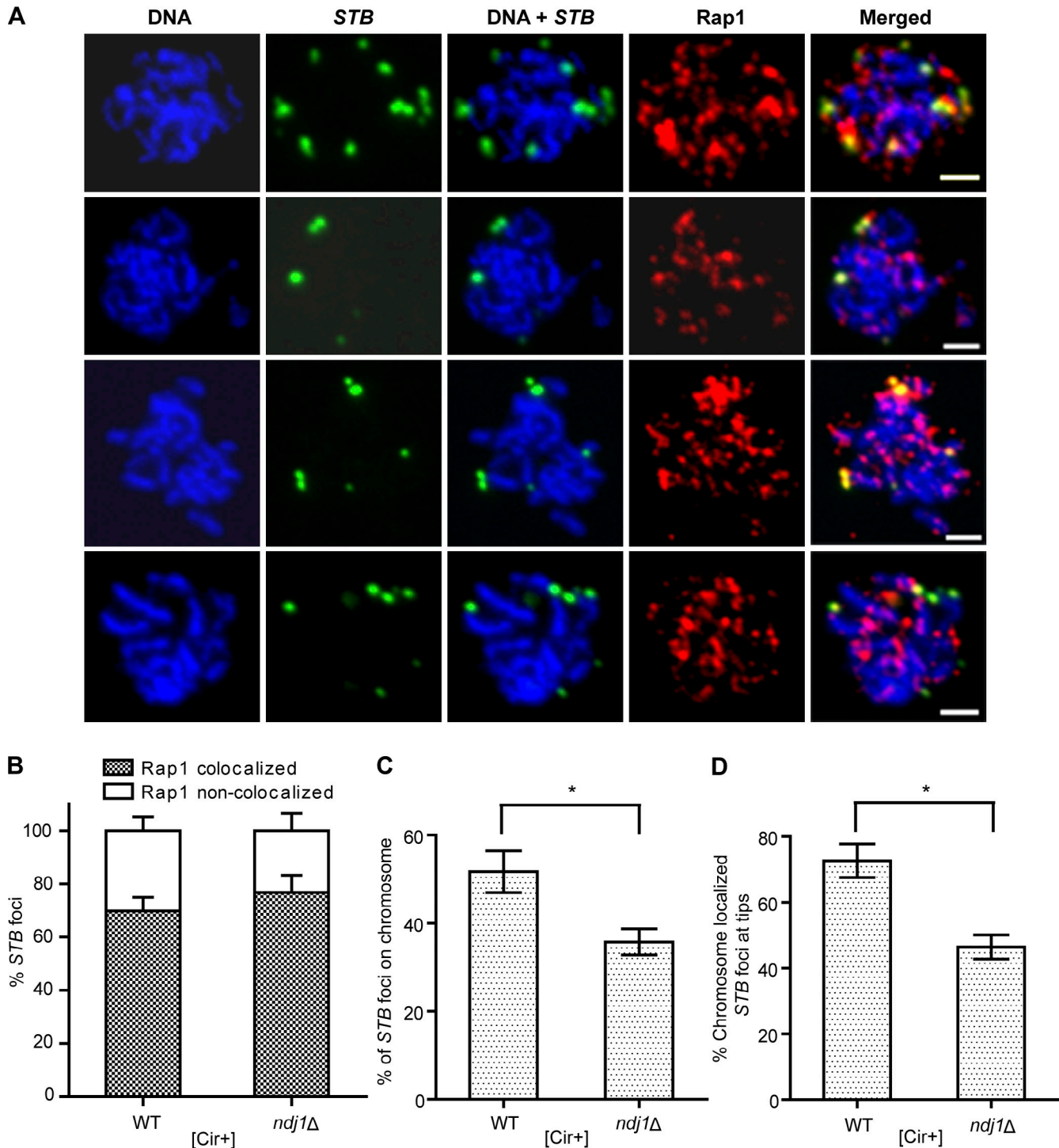
Figure 9. **Localization of *STB* plasmid foci with respect to Rap1 in the *ndj1Δ* strain.** (A) Chromosome spreads prepared from pachytene stage cells of the *ndj1Δ* strain (at 7.5 h into meiosis) were assayed for the fraction of *STB* plasmid foci colocalized with Rap1 foci (B) and that associated with chromosomes (C). Within the latter class, plasmid foci located at chromosome tips were demarcated (D). These data were collected by screening 22 spreads comprising 180 plasmid foci. The histograms for the wild-type strain in B–D were taken from Fig. 3 H (5.5 h), Fig. 2 D, and Fig. 2 E, respectively. The error bars indicate ± SEM. *, P < 0.05 (two-tailed *t* test). Bars, 2 μm.

Conditional mutations that perturb chromosome segregation without affecting spindle pole body or spindle functions cause 2 micron plasmid missegregation (Velmurugan et al., 2000;

Mehta et al., 2002). Unlike *CEN*, two copies of *STB* in cis do not lead to plasmid instabilities (unpublished data). The nuclear distribution of *STB* plasmid foci in mitotic cells does not

occurrence (33.3%) of a plasmid focus within a zone. The experimental strains harbored fluorescence-tagged *CEN VII* (TetR-Td-Tomato-[TetO]$_{224}$) (red dot). Leptotene/zygotene and pachytene stages were distinguished by two red dots (unpaired homologues; cohesed sisters) and one red dot (paired homologues), respectively. The data in all panels were each obtained by analyzing ~100 plasmid foci. Bars, 2 μm.

Figure 10. **Meiosis plasmid segregation in *ndj1Δ* and *csm4Δ* strains: A model for 2 micron plasmid segregation during meiosis I.** The segregation analyses were performed using the *STB* reporter plasmid, as described under Fig. 1. The bar graphs showing the types of plasmid segregation during meiosis I (A) represent the analysis of 75–100 cells. Wild-type values are from Fig. 1 C. The n:~n class includes n:n and n:n − 1. Segregation results for a chromosome, fluorescence-tagged at *CEN* on both homologues, are given in Fig. S5. (B) A model embodying current results envisages the 2 micron plasmid as gaining access to the nuclear envelope-associated motor machinery with the assistance of the Rep1-Rep2-*STB* system. Ndj1 appears not to be essential for plasmid–membrane association, although it may enhance plasmid tethering to *TEL*s as they become anchored at the envelope and engage the motor. An alternative membrane-independent interaction of plasmids with *TEL*s (shown by the broken lines) cannot be ruled out. Csm4, the force transducer of the motor, may be related to KASH domain proteins (Koszul and Kleckner, 2009). *TEL*-associated plasmid segregation during meiosis I would be consistent with potential hitchhiking of plasmids on chromosomes during mitosis (Velmurugan et al., 2000; Mehta et al., 2002; Liu et al., 2013). Current evidence does not preclude meiotic plasmid segregation in a membrane-associated fashion independent of chromosomes. Furthermore, the *TEL*-associated and chromosome-independent pathways of plasmid segregation need not be mutually exclusive. The representations of Csm4 and Mps3 here are patterned after those from an earlier review (Starr and Fridolfsson, 2010).
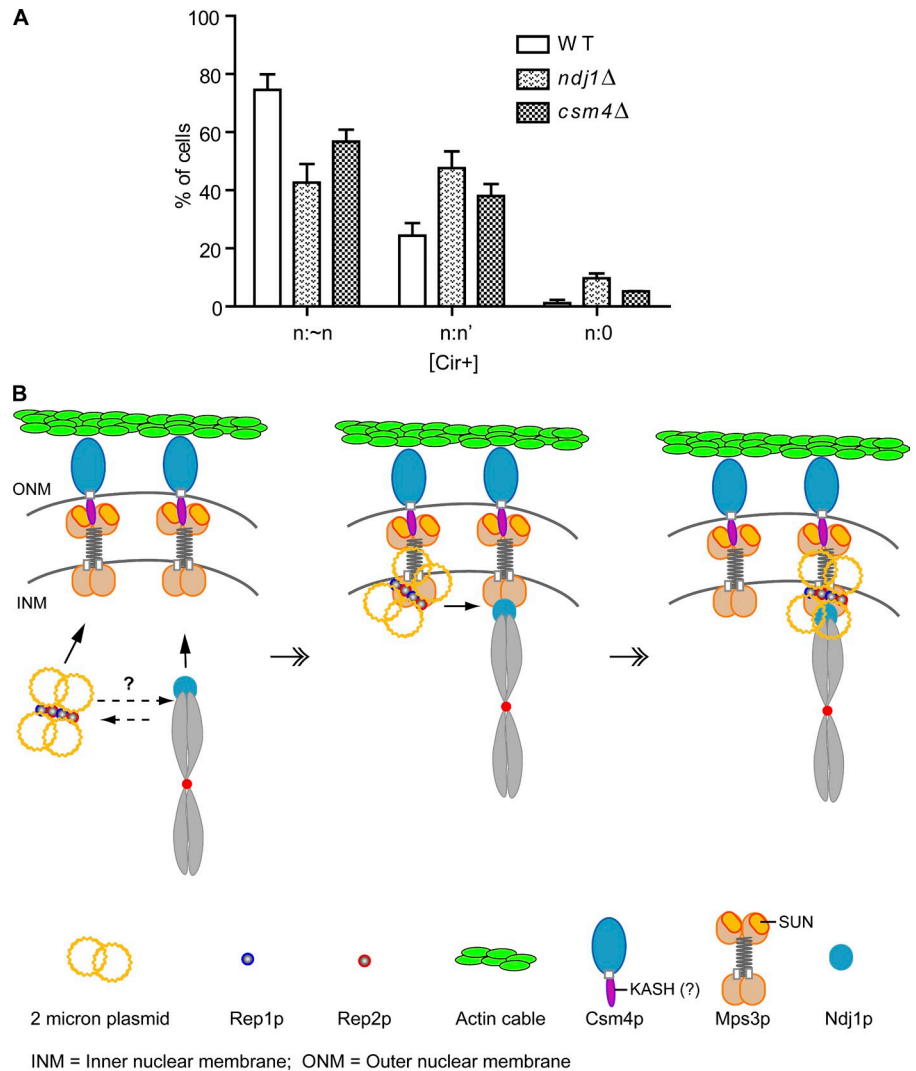
reveal preferred plasmid localization at the periphery (Heun et al., 2001; Mehta et al., 2005). Cumulative evidence is consistent with the plasmid overcoming mother bias by hitchhiking on chromosomes (Velmurugan et al., 2000; Mehta et al., 2002; Liu et al., 2013). Tethering to chromosomes for stable maintenance in host cells is a strategy that viral episomes of the gammaherpes and papilloma families resort to as well (Wu et al., 2000; McBride et al., 2004; You et al., 2004).

If the meiotic segregation of the 2 micron plasmid is coupled to chromosome segregation, the plasmid has to adapt to the reductional division of meiosis I, when chromosome homologues, but not sister chromatids, separate from each other. Plasmid segregation during meiosis II may be mechanistically analogous to that during mitosis. The seminal findings from the present study are (a) repositioning of an *STB* reporter plasmid to the nuclear periphery as cells enter the meiotic program, (b) localization of plasmid foci at or close to *TEL*s, (c) potential plasmid interaction with the nuclear envelope motor that also engages *TEL*s, (d) similarities in motor-driven plasmid and *TEL* dynamics during prophase I, and (e) the requirement of the motor-associated proteins Ndj1 and Csm4 for normal meiotic segregation of the plasmid.

Collectively, they are consistent with motor-assisted and *TEL*-associated segregation of the 2 micron plasmid during meiosis I (Fig. 10 B).

Association of the 2 micron plasmid with the envelope motor and *TEL*s during meiosis I

The localization patterns of the *STB* reporter plasmid and of Rep1 with respect to chromosomes, Mps3, and Rap1 are consistent with the Rep1-Rep2–assisted interaction of the 2 micron plasmid with *TEL*s and/or the envelope motor. This interaction may be stabilized by the membrane anchoring of *TEL*s and their association with the motor, as suggested by the increase in the fraction of Rap1- or Mps3-associated plasmid foci at pachytene.

The relocation of *STB* plasmid foci from the interior of the nuclei in mitotic cells (Heun et al., 2001; Mehta et al., 2005) to the nuclear periphery in meiotic cells (this study) suggests that the plasmid may be stationed at distinct chromosome sites during the two cell cycle programs. Csm4 and Ndj1 are meiosis specific (Burns et al., 1994; Chua and Roeder, 1997; Conrad et al., 1997; Chu et al., 1998; Primig et al., 2000; Rabitsch et al., 2001), whereas Mps3 levels increase markedly at the onset of meiosis

(Conrad et al., 2007). Difference in the host proteins that mediate plasmid–chromosome association may account for potentially distinct plasmid tethering sites in mitotic versus meiotic cells.

The envelope motor that triggers rapid *TEL* movements also promotes 2 micron plasmid dynamics and segregation during meiosis I

The *TEL*-like prophase movements and equal meiosis I segregation of the *STB* reporter plasmid are dependent on Csm4 and Ndj1. Whereas rapid chromosome movements serve critical functions in the faithful segregation of homologues (Kosaka et al., 2008; Koszul et al., 2008; Wanat et al., 2008; Lee et al., 2012), a role for motor-driven dynamics themselves in plasmid segregation is hard to conceive. More likely, plasmid association with the motor segues into plasmid tethering to *TEL*s and thus plasmid segregation by hitchhiking. However, coordinated plasmid and *TEL* movements may be conducive to their mutual association. If the plasmid-associated motor components are evenly partitioned, they would provide vehicles for equal plasmid segregation. It is not known how Csm4, Ndj1, and Mps3 are distributed at the end of meiosis I. Alternative plasmid segregation mechanisms, both membrane-associated and chromosome-associated, need not be mutually exclusive.

The mother bias of *ARS* plasmids has been attributed to the geometry of the nucleus, with its constricted neck and the relatively short duration of mitosis, or perhaps to a more direct barrier to plasmid diffusion, all of which would impede mother–daughter equilibration of plasmid molecules (Shcheprova et al., 2008; Gehlen et al., 2011). The diffusion barrier can be at least partially overcome by tethering multicopy *ARS* plasmids to certain nuclear pore proteins, to the nuclear envelope, or to *TEL*-associated proteins (Gehlen et al., 2011; Khmelinskii et al., 2011). The nuclear organization during meiosis I has no apparent geometric bottleneck; yet, the *ARS* reporter plasmid experiences high missegregation (∼57%) and significant failed segregation (∼14%) events. Additional nongeometric constraints, such as the aggregation of plasmid molecules and/or plasmid interactions with multiprotein assemblies or with subnuclear structures, may interfere with passive plasmid segregation.

The model for plasmid–*TEL* coupling: Implications and limitations

While the model presented in Fig. 10 B is heuristic, the details will need to be refined. Because chromosome segregation is affected by *ndj1Δ* and *csm4Δ*, missegregation of the plasmid in these mutants can be explained, at least partly, by its association with chromosomes. Despite defective chromosome dynamics and meiotic progression, the mutants are at least 50% as efficient as the wild type in sporulation, with >60% spore viability (Conrad et al., 2008; Kosaka et al., 2008). There must be salvage pathways that rescue meiosis with moderate competence. In the current model, *ndj1Δ* reduces the efficiency of plasmid segregation by blocking access to *TEL*s, as their membrane anchoring is destabilized. In contrast, *csm4Δ* does not seem to perturb *TEL* localization at the envelope (Conrad et al., 2008; Kosaka et al., 2008; Wanat et al., 2008). Csm4 is required for bouquet formation, which may facilitate plasmid–chromosome

interactions. The *csm4Δ* effect on plasmid segregation may be largely indirect, and manifest through chromosome segregation. However, subtle changes in plasmid positioning due to the defective MNC complex, as well as subdued plasmid and/or chromosome mobility, may hinder plasmid–*TEL* docking.

Meiotic segregation of the 2 micron plasmid: Logic for chromosome association?

Assuming that the hitchhiking model applies to meiosis I, it is not clear what advantage *TEL*s might offer over other chromosomal locales as plasmid tethering sites. Chromosome termini, being generally bereft of genes, may provide safe plasmid homing sites without disrupting normal gene expression and/or regulation. Infrequent double-strand breaks and low meiotic recombination frequencies at subtelomeric regions may lower the likelihood of plasmid dislodgement by assembly of the recombination–repair machinery and its DNA processing activities.

Equal plasmid segregation in association with *TEL*s during meiosis I (and perhaps meiosis II as well) would demand a very specialized high-order organization of replicated molecules within a *TEL*-associated plasmid focus. Furthermore, this organization has to be refractory to chromosomal exchanges by recombination. If a plasmid focus were composed of four equivalent segregation units, each tethered to one of the four *TEL*s of a homologue pair, plasmid segregation would follow the 2:2 rule during meiosis I and the 1:1 rule during meiosis II.

In a simpler model of random plasmid–*TEL* association, each plasmid focus would cosegregate with a pair of sister chromatids to one of the two daughter nuclei during meiosis I. For the 6–8 plasmid foci normally observed per cell, the probability of plasmid loss from a nucleus would be quite low: ∼3% $[(0.5)^6 \times 2]$ and ∼0.8% $[(0.5)^8 \times 2]$, for the 6 and 8 foci cases, respectively. However, the corresponding equal segregation frequencies, 3:3 and 4:4, would be only ∼31% and ∼27%, respectively. In principle, a decrease in plasmid copy number resulting from this type of segregation may be rectified subsequently by Flp-mediated amplification (Futcher, 1986; Volkert and Broach, 1986). However, amplification is seldom triggered during normal steady-state mitotic growth, with nearly every 2 micron plasmid molecule replicating once, and only once, during an S phase (Zakian et al., 1979). It is not known whether a replication control mechanism counteracts a higher-than-normal plasmid copy number within a nucleus. Cells containing very high plasmid copy numbers would be eliminated over time because of the selective disadvantage they suffer from plasmid overload (Holm, 1982; Chen et al., 2005, 2007; Dobson et al., 2005).

Single-copy derivatives of *STB* reporter plasmids have been successfully exploited to address the mitotic segregation of the 2 micron plasmid without the uncertainties introduced by multiple plasmid copies (Ghosh et al., 2007; Liu et al., 2013). Analogous reporters would be equally helpful in unveiling the segregation behavior of plasmid sisters during meiosis I.

Materials and methods

Strains and plasmids
Strains and plasmids used in this study are listed in Table S1 and Table S2. The relevant genotypes of strains as well as appropriate references are

included. Strains carrying endogenous 2 micron plasmid are designated as [cir+], whereas those cured of the plasmid are indicated as [cir0]. The diploid strains for plasmid segregation, localization, and dynamics assays were constructed anew for each set of assays. The reporter plasmid was introduced into the desired "a" mating type strain by transformation, and the transformant was mated with the "α" mating type partner strain. Strains and plasmids were provided by A. Murray (Harvard University, Cambridge, MA), A. Johnson (University of Texas at Austin, Austin, TX), and E. Alani (Cornell University, Ithaca, NY) served as templates for the construction of a subset of those listed in Table S1 and Table S2.

Genomic manipulations
Genetic modifications at desired chromosomal locales were introduced by previously published procedures (Longtine et al., 1998). They were confirmed by PCR, Southern analysis, and, in the case of epitope addition, by Western blotting. C-terminal tags of 3-HA and 13-Myc were introduced at the MPS3 and CTF19 loci, respectively, in strains used for immunofluorescence assays. DNA sequences corresponding to amino acids 20–282 of Ndj1 or 20–140 of Csm4 were deleted by KANMX6 insertion at the corresponding native locus. Mutant strains used in plasmid and chromosome dynamics assays were constructed by replacing DNA sequences corresponding to amino acids 14–252 of Ndj1 or 27–156 of Csm4 by TRP1 (Berben et al., 1991). Expression cassettes for GFP-LacI were integrated at URA3 (under the control of the HIS3 promoter) and at LYS2 (under the control of the DMC1 promoter) for visualizing reporter plasmids harboring a [LacO]$_{256}$ array. A derivative of plasmid pRS404 (Sikorski and Hieter, 1989) containing [TetO]$_{224}$ and a CEN proximal segment of chromosome VII (between coordinates 479055 and 479542) or the left TEL segment of chromosome VII (between coordinates 4025 and 5037) was inserted at the corresponding chromosome location by homologous recombination. An expression vector for TetR-tdTomato (controlled by the URA3 promoter; Matos et al., 2008), modified by disrupting LEU2 by TYR1, was inserted at TYR1 to tag the TetO repeats by red fluorescence.

Meiotic regimen
Synchronization of meiotic cultures was performed as described previously (Dresser et al., 1997). In brief, fresh diploids obtained by mating the pertinent haploid strains were grown for ∼20 h in selective medium for maintaining the resident reporter plasmid. An aliquot of the cells was transferred to YPA medium (1% yeast extract, 2% Bacto Peptone, and 1% potassium acetate) and grown to a density of 3–5 × 10^7 [cells plus buds]/ml. At this time (deemed as zero for the start of meiosis), they were shifted to sporulation medium (2% potassium acetate supplemented with all essential amino acids, pH 7.0) at 30°C. To minimize background fluorescence from intermediates of adenine biosynthesis during microscopy, all growth media were supplemented with 1.0 mg/ml adenine.

Timing of cytological and dynamics assays
The wild-type and mutant strains used for this study have been extensively characterized with respect to the kinetics of completion of individual stages of meiosis under the conditions specified in the preceding paragraph (Conrad et al., 2007, 2008). Furthermore, in all of the cytological assays, the meiotic stage was verified by the pattern of Zip1 staining in chromosome spreads. For the wild-type strain, 3.5–4 h in sporulation medium corresponded to the leptotene/zygotene stage, with Zip1 present mostly as spots (foci) along with a few short stretches indicating partial synapsis. The pachytene stage (5.5 h) was characterized by elongated Zip1 filaments, nearly all stretching end-to-end along paired chromosomes (DAPI stained). The ndj1Δ and csm4Δ mutants were at the early zygotene stage at 4 h. The 7–8-h and 7–10-h intervals marked the pachytene stage in the ndj1Δ and csm4Δ strains, respectively.

Segregation assays
The multicopy STB and ARS reporter plasmids used in the segregation assays were similar in size and organization, and contained the [LacO]$_{256}$ array with LEU2 as the selectable marker (Table S2). The STB and ARS reporters harbored early firing replication origins: the 2 micron plasmid origin and ARS1, respectively. Previous studies showed that the segregation status of a single copy or a multicopy STB plasmid is unaffected, whether the source of Rep proteins is the endogenous 2 micron plasmid of a [cir+] strain or a [cir0] strain engineered to express these proteins (Velmurugan et al., 2000; Ghosh et al., 2007; Liu et al., 2013). Furthermore, sisters formed from replication of a single-copy plasmid segregate away from each other. Assuming that this functional organization of plasmid foci is not grossly altered in meiosis, the native 2 micron plasmid molecules (which remain invisible in the segregation assays) will not be competing with the

STB reporter plasmid. If such competition were to occur, we would be underestimating the equal segregation frequencies of the latter.

Meiosis I and II were identified by cells with distinct two and four DAPI-stained lobes (nuclei), respectively (Fig. 1, Fig. 10, Fig. S1, and Fig. S5). Green fluorescent foci denoting a reporter plasmid (bound by GFP-LacI) and red fluorescent foci denoting a reporter chromosome (bound by TetR-tdTomato) were counted in individual nuclei.

Preparation of fixed cells
Cells were fixed in 4% PFA for 10 min at room temperature, washed once with 0.1 M phosphate buffer, pH 7.5, containing 1.2 M sorbitol, and resuspended in the same buffer. For nuclear staining, Triton X-100 was added to a final concentration of 0.1% and incubated for 5 min at room temperature. After addition of DAPI (0.8 μg/ml) and 1 min of incubation, cells were washed three times with cold PBS, pH 7.4, and resuspended in the same buffer. They were spread onto glass slides and imaged as described under "Fluorescence microscopy."

Chromosome spreads
Spheroplasts obtained as described in Dresser and Giroux (1988) were used for preparing nuclear (chromosome) spreads according to previously published methods (Voelkel-Meiman et al., 2012). In brief, 10 ml of a culture at a given stage of meiosis was resuspended in 2 ml of ZK buffer (25 mM Tris, pH 7.5, and 0.8 M KCl) and treated with 40 μl of 1 M DTT for 2 min. Cells were resuspended in 2 ml of ZK buffer and incubated with 15 μl of zymolase solution for 30 min at 30°C to obtain spheroplasts. Spheroplasts were pelleted, washed with cold MES/Sorbitol solution (0.1 M MES-NaOH, pH 6.4, 1 mM EDTA, 0.5 mM MgCl$_2$, and 1 M Sorbitol), resuspended in the same buffer, and kept in ice. One half or one fourth of the spheroplast solution was pelleted, and 80 μl of 1× MES as well as 200 μl of 4% paraformaldehyde were added. 100–140 μl of the resuspended spheroplast solution was applied directly onto a clean superfrost plus slide (catalog No. 12-550-15; Thermo Fisher Scientific) and distributed over its entire surface using the edge of a coverslip. The slide was allowed to air dry at least for 20 min before washing it with 0.4% Photo-Flo (0.4% vol/vol solution of Photo-Flo 200 solution [Kodak] in sterile water). The spreads were used for visualizing chromosomes by DAPI staining or proteins by treating with specific antibodies followed by indirect immunofluorescence.

Antibodies
The following primary antibodies were used: mouse anti-GFP (1:300), goat anti-Myc (1:300), rabbit anti-HA (1:300), rabbit anti-RFP (1:300; all from Abcam), rabbit anti-Zip1 (1:100; a generous gift from S. Roeder, Yale University, New Haven, CT), and rabbit anti-Rep1 (1:200; Velmurugan et al., 2000). The secondary antibodies used were: donkey anti–mouse FITC (1:200) and goat anti–rabbit Texas red (1:200 and 1:400) from Jackson ImmunoResearch Laboratories, Inc., and donkey anti–goat Alexa Fluor 568 (1:500) from Invitrogen.

Fluorescence microscopy
Images were captured at room temperature in 0.4-μm (Fig. 1, Fig. 10, Fig. S1, and Fig. S5) and 0.2-μm (all other figures) z sections, with a pixel spacing of 0.129 μm using a microscope (BX-60; Olympus) with a 100× oil immersion objective lens (NA 1.3) and a camera (Photometrix Quantix; Roper Scientific). MetaMorph 7.5 software (Molecular Devices) was used for image analysis. Image stacks covering at least 4 μm of the nucleus were deconvolved using MetaMorph 2D deconvolution software using nearest neighbors algorithm.

Time-lapse video microscopy
Time-lapse video microscopy was performed as previously described by Conrad et al. (2008). The movements of reporter plasmids (Fig. 5, Fig. 6, Fig. S2, Fig. S3, and Fig. S4) were analyzed using the custom software OMRFQANT (Conrad et al., 2008). The assays with the fluorescence-tagged STB reporter plasmid (green) in the wild-type strain also included fluorescence-tagged chromosome VIII TEL (red) for reference. In the series of video frames captured at a rate of 1 frame/s, alternate frames represented the plasmid and TEL, respectively. Therefore histogram plots for the dynamics of the STB plasmid in the wild-type strain corresponded to 1 frame/2 s. The movements of the STB plasmid in the ndj1Δ and csm4Δ strains were followed at 1 frame/s. The data for paired and unpaired TELs and for the CEN-ARS-TEL plasmid in the wild-type and mutant strains were also obtained at 1 frame/s. In those plots that included the STB plasmid in the wild-type strain (Fig. 5, A–I; Fig. 6, A–C; and Fig. S3, A–C), all the 1 frame/s datasets were converted to 1 frame/2 s (by skipping alternate frames). By doing so,

the time resolution was kept constant for every pairwise comparison. However, this manipulation had the effect of altering the histogram patterns for the same dataset between different panels of a given figure, for example, the mean and maximum speeds of the *STB* plasmid in A and B versus D and E, respectively, of Fig. 6. The difference arises because the sum of the vectorial displacements AB and BC recorded over two 1-s intervals will not equal AC (unless the points ABC form a straight line), the resultant displacement when the movements are recorded over a 2-s interval. Because, by triangle inequality, AC < AB + BC, the same set of movements will appear slightly slower in a 1 frame/2 s plot compared with 1 frame/s plot.

Paired and unpaired *TEL*s were distinguished as one spot and two spots, respectively (Fig. S3). In the few instances when this distinction was not as clear-cut, a *TEL* appearing as two spots in >6 frames out of 60 frames (in 1 frame/s movies) was defined as unpaired.

Mapping reporter plasmid or Rep1 foci with respect to chromosomes using fluorescence signals in cytological assays

The following rules were applied for mapping an *STB* reporter plasmid with respect to chromosomes marked by DAPI (or by Zip1) in pachytene stage nuclear spreads (Fig. 2 and Fig. 9). If the plasmid was closer to the arm (lateral location) than to the tip (end location) of a chromosome, the distance between the centroid (the brightest pixel) of the plasmid focus and the brightest chromosome pixel closest to it was registered. In the few instances when the brightest chromosome pixel could not be assessed unambiguously (intensity difference of <5%), the more peripheral one was chosen to represent the chromosome edge. For mapping a plasmid focus located proximal to a chromosome tip, the end of a chromosome was defined based on the intensity changes in the longitudinal array of DAPI pixels lining it. The brightest row of pixels marking nearly the entire chromosome length showed little variation in intensity (within 2–5%). Near the ends however, the pixels became progressively fainter, making it difficult to precisely determine the boundary. The last pixel of the series beyond which the intensity fell 10% or more was taken to be located at the chromosome end. The "end" group of pixels was then delimited by the constraint that the intensity of an included pixel could not drop by >5% of that of its brightest member. Further steps were the same as those for the lateral distance measurements. Namely, the separation of the centroid of a plasmid focus from the nearest pixel representing the chromosome end was determined. The mapping procedure applied to plasmid foci was also used in measuring the distances of Rep1 foci from chromosomes (Fig. 4).

Criteria for colocalization of two fluorescence-tagged nuclear entities in cytological assays

The signals from two fluorescent foci (green in one case and red in the other) were defined as colocalized if they overlapped almost perfectly to generate a yellow signal or partially overlapped to generate a green-yellow-red/green-yellow/red-yellow signal (Fig. 3, Fig. 4, and Fig. 9). As the resolution at a single pixel level corresponds to 0.129 µm and as there is occasional ambiguity in deciding the centroid pixel within a signal, complete coincidence and partial coincidence in our estimates indicate a spacing of 0.0–0.26 µm (2 pixels) and 0.26–0.39 µm (3 pixels), respectively.

Mapping a reporter plasmid focus with respect to the nuclear boundary using fluorescence signals in cytological assays

The distances of plasmid foci from the nuclear boundary (Fig. 8, A–C) in fixed cells, which are assumed to preserve the overall three-dimensional organization of nuclei, were measured as follows. First, image stacks of a nucleus stained with DAPI were generated from slices with a step size of 0.2 µm. As the multiple plasmid foci were not coplanar in their locations, the z sections that captured the highest intensity from each individual plasmid signal were identified. The shortest distance from the plasmid centroid (the brightest pixel signifying the center of the plasmid focus) to the brightest DAPI pixel at the edge of the same image plane (nuclear boundary) was measured.

Localization of a plasmid focus with respect to the Nup49-mCherry signal demarcating the nuclear boundary (Fig. 8, D and E) was performed as follows. Plasmid foci situated within 20% of the focal planes from each pole were excluded from the analysis, as Nup49-mCherry signals were poorly resolved near the poles (Meister et al., 2010). Furthermore, the Nup49 fluorescence signals were often discontinuous and nonuniform in size. The local membrane contour within an image plane was traced along the midpoints between the inner and outer edges of the relevant signals (Mehta et al., 2005). Adjacent traces were connected by smooth curves in regions lacking the Nup49 signal. The line signifying the shortest distance of a plasmid focus from the membrane was extended to the opposite membrane arc to obtain the diameter of the nuclear cross section. Each focus was assigned to one of three zones of equal areas based on its distance from the edge normalized to the radius, as described previously (Meister et al., 2010). As the cross sections of the meiotic nuclei were often locally distorted from circularity, the radius was not constant among the different plasmid foci. However, this did not affect the zonal allocation of the foci as a function of the radius.

Other miscellaneous protocols

Standard protocols for yeast and bacterial transformations, yeast DNA and plasmid DNA preparation, curing [cir+] strains of the endogenous 2 micron plasmid to generate corresponding [cir0] strains, culturing yeast and bacteria, and other routine procedures have been published previously (Velmurugan et al., 2000; Liu et al., 2013).

Online supplemental material

Fig. S1 shows *STB* and *ARS* plasmid distribution in spores, and classification of tetrads containing plasmid foci in all four spores. Fig. S2 shows plasmid dynamics in *csm4Δ* and *ndj1Δ* strains at 4 h after transfer to sporulation medium. Fig. S3 shows *TEL* and *STB* plasmid dynamics in the wild-type and *ndj1Δ* strains. Fig. S4 shows dynamics of a *CEN-ARS* plasmid in the wild type, *ndj1Δ*, and *csm4Δ* strains. Fig. S5 shows plasmid distribution in tetrads and chromosome segregation in the *ndj1Δ* and *csm4Δ* strains. Tables S1 and S2 show strains and plasmids used in this study. Video 1 (related to Fig. 5, A–F; and Fig. 6, D–I) shows chromosome dynamics in wild-type and *csm4Δ* cells. Video 2 (related to Fig. 5, A–I; Fig. 6, A–I; and Fig. S3, A–C) shows *STB* plasmid dynamics in wild-type and *csm4Δ* cells. Video 3 (related to Fig. S3, D–I) shows chromosome dynamics in wild-type and *ndj1Δ* cells. Video 4 (related to Fig. S3, A–I) shows *STB* plasmid dynamics in wild-type and *ndj1Δ* cells. Online supplemental material is available at http://www.jcb.org/cgi/content/full/jcb.201312002/DC1. Additional data are available in the JCB DataViewer at http://dx.doi.org/10.1083/jcb.201312002.dv.

References

Baker, B.S., A.T.C. Carpenter, M.S. Esposito, R.E. Esposito, and L. Sandler. 1976. The genetic control of meiosis. *Annu. Rev. Genet.* 10:53–134. http://dx.doi.org/10.1146/annurev.ge.10.120176.000413

Berben, G., J. Dumont, V. Gilliquet, P.-A. Bolle, and F. Hilger. 1991. The YDp plasmids: a uniform set of vectors bearing versatile gene disruption cassettes for *Saccharomyces cerevisiae*. *Yeast*. 7:475–477. http://dx.doi.org/10.1002/yea.320070506

Brewer, B.J., and W.L. Fangman. 1980. Preferential inclusion of extrachromosomal genetic elements in yeast meiotic spores. *Proc. Natl. Acad. Sci. USA*. 77:5380–5384. http://dx.doi.org/10.1073/pnas.77.9.5380

Burns, N., B. Grimwade, P.B. Ross-Macdonald, E.Y. Choi, K. Finberg, G.S. Roeder, and M. Snyder. 1994. Large-scale analysis of gene expression, protein localization, and gene disruption in *Saccharomyces cerevisiae*. *Genes Dev.* 8:1087–1105. http://dx.doi.org/10.1101/gad.8.9.1087

Chen, X.L., A. Reindle, and E.S. Johnson. 2005. Misregulation of 2µm circle copy number in a SUMO pathway mutant. *Mol. Cell. Biol.* 25:4311–4320. http://dx.doi.org/10.1128/MCB.25.10.4311-4320.2005

Chen, X.L., H.R. Silver, L. Xiong, I. Belichenko, C. Adegite, and E.S. Johnson. 2007. Topoisomerase I-dependent viability loss in s*accharomyces cerevisiae* mutants defective in both SUMO conjugation and DNA repair. *Genetics*. 177:17–30. http://dx.doi.org/10.1534/genetics.107.074708

Chu, S., J. DeRisi, M. Eisen, J. Mulholland, D. Botstein, P.O. Brown, and I. Herskowitz. 1998. The transcriptional program of sporulation in budding yeast. *Science*. 282:699–705. http://dx.doi.org/10.1126/science.282.5389.699

Chua, P.R., and G.S. Roeder. 1997. Tam1, a telomere-associated meiotic protein, functions in chromosome synapsis and crossover interference. *Genes Dev.* 11:1786–1800. http://dx.doi.org/10.1101/gad.11.14.1786

Conrad, M.N., A.M. Dominguez, and M.E. Dresser. 1997. Ndj1p, a meiotic telomere protein required for normal chromosome synapsis and segregation in yeast. *Science*. 276:1252–1255. http://dx.doi.org/10.1126/science.276.5316.1252

Conrad, M.N., C.-Y. Lee, J.L. Wilkerson, and M.E. Dresser. 2007. MPS3 mediates meiotic bouquet formation in *Saccharomyces cerevisiae*. *Proc. Natl. Acad. Sci. USA*. 104:8863–8868. http://dx.doi.org/10.1073/pnas.0606165104

Conrad, M.N., C.-Y. Lee, G. Chao, M. Shinohara, H. Kosaka, A. Shinohara, J.A. Conchello, and M.E. Dresser. 2008. Rapid telomere movement in meiotic prophase is promoted by NDJ1, MPS3, and CSM4 and is modulated by recombination. *Cell*. 133:1175–1187. http://dx.doi.org/10.1016/j.cell.2008.04.047

Cui, H., S.K. Ghosh, and M. Jayaram. 2009. The selfish yeast plasmid uses the nuclear motor Kip1p but not Cin8p for its localization and equal segregation. *J. Cell Biol*. 185:251–264. http://dx.doi.org/10.1083/jcb.200810130

Dobson, M.J., A.J. Pickett, S. Velmurugan, J.B. Pinder, L.A. Barrett, M. Jayaram, and J.S.K. Chew. 2005. The 2μm Plasmid Causes Cell Death in *Saccharomyces cerevisiae* with a Mutation in Ulp1 Protease. *Mol. Cell. Biol*. 25:4299–4310. http://dx.doi.org/10.1128/MCB.25.10.4299-4310.2005

Dresser, M.E., and C.N. Giroux. 1988. Meiotic chromosome behavior in spread preparations of yeast. *J. Cell Biol*. 106:567–573. http://dx.doi.org/10.1083/jcb.106.3.567

Dresser, M.E., D.J. Ewing, M.N. Conrad, A.M. Dominguez, R. Barstead, H. Jiang, and T. Kodadek. 1997. DMC1 functions in a *Saccharomyces cerevisiae* meiotic pathway that is largely independent of the RAD51 pathway. *Genetics*. 147:533–544.

Futcher, A.B. 1986. Copy number amplification of the 2 μm circle plasmid of *Saccharomyces cerevisiae*. *J. Theor. Biol*. 119:197–204. http://dx.doi.org/10.1016/S0022-5193(86)80074-1

Gehlen, L.R., S. Nagai, K. Shimada, P. Meister, A. Taddei, and S.M. Gasser. 2011. Nuclear geometry and rapid mitosis ensure asymmetric episome segregation in yeast. *Curr. Biol*. 21:25–33. http://dx.doi.org/10.1016/j.cub.2010.12.016

Ghosh, S.K., S. Hajra, A. Paek, and M. Jayaram. 2006. Mechanisms for chromosome and plasmid segregation. *Annu. Rev. Biochem*. 75:211–241. http://dx.doi.org/10.1146/annurev.biochem.75.101304.124037

Ghosh, S.K., S. Hajra, and M. Jayaram. 2007. Faithful segregation of the multicopy yeast plasmid through cohesin-mediated recognition of sisters. *Proc. Natl. Acad. Sci. USA*. 104:13034–13039. http://dx.doi.org/10.1073/pnas.0702996104

Ghosh, S.K., C.-C. Huang, S. Hajra, and M. Jayaram. 2010. Yeast cohesin complex embraces 2 micron plasmid sisters in a tri-linked catenane complex. *Nucleic Acids Res*. 38:570–584. http://dx.doi.org/10.1093/nar/gkp993

Hajra, S., S.K. Ghosh, and M. Jayaram. 2006. The centromere-specific histone variant Cse4p (CENP-A) is essential for functional chromatin architecture at the yeast 2-μm circle partitioning locus and promotes equal plasmid segregation. *J. Cell Biol*. 174:779–790. http://dx.doi.org/10.1083/jcb.200603042

Heun, P., T. Laroche, M.K. Raghuraman, and S.M. Gasser. 2001. The positioning and dynamics of origins of replication in the budding yeast nucleus. *J. Cell Biol*. 152:385–400. http://dx.doi.org/10.1083/jcb.152.2.385

Holm, C. 1982. Clonal lethality caused by the yeast plasmid 2 μ DNA. *Cell*. 29:585–594. http://dx.doi.org/10.1016/0092-8674(82)90174-X

Hsiao, C.L., and J. Carbon. 1981. Direct selection procedure for the isolation of functional centromeric DNA. *Proc. Natl. Acad. Sci. USA*. 78:3760–3764. http://dx.doi.org/10.1073/pnas.78.6.3760

Huang, C.-C., K.-M. Chang, H. Cui, and M. Jayaram. 2011a. Histone H3-variant Cse4-induced positive DNA supercoiling in the yeast plasmid has implications for a plasmid origin of a chromosome centromere. *Proc. Natl. Acad. Sci. USA*. 108:13671–13676. http://dx.doi.org/10.1073/pnas.1101944108

Huang, C.-C., S. Hajra, S.K. Ghosh, and M. Jayaram. 2011b. Cse4 (CenH3) association with the Saccharomyces cerevisiae plasmid partitioning locus in its native and chromosomally integrated states: implications in centromere evolution. *Mol. Cell. Biol*. 31:1030–1040. http://dx.doi.org/10.1128/MCB.01191-10

Hyland, K.M., J. Kingsbury, D. Koshland, and P. Hieter. 1999. Ctf19p: A novel kinetochore protein in *Saccharomyces cerevisiae* and a potential link between the kinetochore and mitotic spindle. *J. Cell Biol*. 145:15–28. http://dx.doi.org/10.1083/jcb.145.1.15

Jayaram, M., S. Mehta, D. Uzri, and S. Velmurugan. 2004a. Segregation of the yeast plasmid: similarities and contrasts with bacterial plasmid partitioning. *Plasmid*. 51:162–178. http://dx.doi.org/10.1016/j.plasmid.2004.02.005

Jayaram, M., X.M. Yang, S. Mehta, Y. Voziyanov, and S. Velmurugan. 2004b. The 2μm plasmid of *Saccharomyces cerevisiae*. *In* Plasmid Biology. B.E. Funnel and G.J. Phillips, editors. ASM Press, Washington, DC. 303–324. http://dx.doi.org/10.1128/9781555817732.ch14

Jayaram, M., K.-M. Chang, C.-H. Ma, C.-C. Huang, Y.-T. Liu, and S. Sau. 2013. Topological similarity between the 2μm plasmid partitioning locus and the budding yeast centromere: evidence for a common evolutionary origin? *Biochem. Soc. Trans*. 41:501–507. http://dx.doi.org/10.1042/BST20120224

Katis, V.L., J. Matos, S. Mori, K. Shirahige, W. Zachariae, and K. Nasmyth. 2004. Spo13 facilitates monopolin recruitment to kinetochores and regulates maintenance of centromeric cohesion during yeast meiosis. *Curr. Biol*. 14:2183–2196. http://dx.doi.org/10.1016/j.cub.2004.12.020

Khmelinskii, A., M. Meurer, M. Knop, and E. Schiebel. 2011. Artificial tethering to nuclear pores promotes partitioning of extrachromosomal DNA during yeast asymmetric cell division. *Curr. Biol*. 21:R17–R18. http://dx.doi.org/10.1016/j.cub.2010.11.034

Klein, F., T. Laroche, M.E. Cardenas, J.F. Hofmann, D. Schweizer, and S.M. Gasser. 1992. Localization of RAP1 and topoisomerase II in nuclei and meiotic chromosomes of yeast. *J. Cell Biol*. 117:935–948. http://dx.doi.org/10.1083/jcb.117.5.935

Klein, F., P. Mahr, M. Galova, S.B.C. Buonomo, C. Michaelis, K. Nairz, and K. Nasmyth. 1999. A central role for cohesins in sister chromatid cohesion, formation of axial elements, and recombination during yeast meiosis. *Cell*. 98:91–103. http://dx.doi.org/10.1016/S0092-8674(00)80609-1

Kosaka, H., M. Shinohara, and A. Shinohara. 2008. Csm4-dependent telomere movement on nuclear envelope promotes meiotic recombination. *PLoS Genet*. 4:e1000196. http://dx.doi.org/10.1371/journal.pgen.1000196

Koszul, R., and N. Kleckner. 2009. Dynamic chromosome movements during meiosis: a way to eliminate unwanted connections? *Trends Cell Biol*. 19:716–724. http://dx.doi.org/10.1016/j.tcb.2009.09.007

Koszul, R., K.P. Kim, M. Prentiss, N. Kleckner, and S. Kameoka. 2008. Meiotic chromosomes move by linkage to dynamic actin cables with transduction of force through the nuclear envelope. *Cell*. 133:1188–1201. http://dx.doi.org/10.1016/j.cell.2008.04.050

Lee, B.H., B.M. Kiburz, and A. Amon. 2004. Spo13 maintains centromeric cohesion and kinetochore coorientation during meiosis I. *Curr. Biol*. 14:2168–2182. http://dx.doi.org/10.1016/j.cub.2004.12.033

Lee, C.Y., M.N. Conrad, and M.E. Dresser. 2012. Meiotic chromosome pairing is promoted by telomere-led chromosome movements independent of bouquet formation. *PLoS Genet*. 8:e1002730. http://dx.doi.org/10.1371/journal.pgen.1002730

Liu, Y.-T., C.-H. Ma, and M. Jayaram. 2013. Co-segregation of yeast plasmid sisters under monopolin-directed mitosis suggests association of plasmid sisters with sister chromatids. *Nucleic Acids Res*. 41:4144–4158. http://dx.doi.org/10.1093/nar/gkt096

Longtine, M.S., A. McKenzie III, D.J. Demarini, N.G. Shah, A. Wach, A. Brachat, P. Philippsen, and J.R. Pringle. 1998. Additional modules for versatile and economical PCR-based gene deletion and modification in *Saccharomyces cerevisiae*. *Yeast*. 14:953–961. http://dx.doi.org/10.1002/(SICI)1097-0061(199807)14:10<953::AID-YEA293>3.0.CO;2-U

Ma, C.-H., H. Cui, S. Hajra, P.A. Rowley, C. Fekete, A. Sarkeshik, S.K. Ghosh, J.R. Yates III, and M. Jayaram. 2013. Temporal sequence and cell cycle cues in the assembly of host factors at the yeast 2 micron plasmid partitioning locus. *Nucleic Acids Res*. 41:2340–2353. http://dx.doi.org/10.1093/nar/gks1338

Malik, H.S., and S. Henikoff. 2009. Major evolutionary transitions in centromere complexity. *Cell*. 138:1067–1082. http://dx.doi.org/10.1016/j.cell.2009.08.036

Marston, A.L., W.-H. Tham, H. Shah, and A. Amon. 2004. A genome-wide screen identifies genes required for centromeric cohesion. *Science*. 303:1367–1370. http://dx.doi.org/10.1126/science.1094220

Matos, J., J.J. Lipp, A. Bogdanova, S. Guillot, E. Okaz, M. Junqueira, A. Shevchenko, and W. Zachariae. 2008. Dbf4-dependent CDC7 kinase links DNA replication to the segregation of homologous chromosomes in meiosis I. *Cell*. 135:662–678. http://dx.doi.org/10.1016/j.cell.2008.10.026

McBride, A.A., M.G. McPhillips, and J.G. Oliveira. 2004. Brd4: tethering, segregation and beyond. *Trends Microbiol*. 12:527–529. http://dx.doi.org/10.1016/j.tim.2004.10.002

Mehta, S., X.M. Yang, C.S. Chan, M.J. Dobson, M. Jayaram, and S. Velmurugan. 2002. The 2 micron plasmid purloins the yeast cohesin complex: a mechanism for coupling plasmid partitioning and chromosome segregation? *J. Cell Biol*. 158:625–637. http://dx.doi.org/10.1083/jcb.200204136

Mehta, S., X.-M. Yang, M. Jayaram, and S. Velmurugan. 2005. A novel role for the mitotic spindle during DNA segregation in yeast: promoting 2μm plasmid-cohesin association. *Mol. Cell. Biol*. 25:4283–4298. http://dx.doi.org/10.1128/MCB.25.10.4283-4298.2005

Meister, P., L.R. Gehlen, E. Varela, V. Kalck, and S.M. Gasser. 2010. Visualizing yeast chromosomes and nuclear architecture. *Methods Enzymol.* 470: 535–567. http://dx.doi.org/10.1016/S0076-6879(10)70021-5

Monje-Casas, F., V.R. Prabhu, B.H. Lee, M. Boselli, and A. Amon. 2007. Kinetochore orientation during meiosis is controlled by Aurora B and the monopolin complex. *Cell.* 128:477–490. http://dx.doi.org/10.1016/j.cell.2006.12.040

Murray, A.W., and J.W. Szostak. 1983. Pedigree analysis of plasmid segregation in yeast. *Cell.* 34:961–970. http://dx.doi.org/10.1016/0092-8674(83)90553-6

Petronczki, M., M.F. Siomos, and K. Nasmyth. 2003. Un ménage à quatre: the molecular biology of chromosome segregation in meiosis. *Cell.* 112:423–440. http://dx.doi.org/10.1016/S0092-8674(03)00083-7

Primig, M., R.M. Williams, E.A. Winzeler, G.G. Tevzadze, A.R. Conway, S.Y. Hwang, R.W. Davis, and R.E. Esposito. 2000. The core meiotic transcriptome in budding yeasts. *Nat. Genet.* 26:415–423. http://dx.doi.org/10.1038/82539

Rabitsch, K.P., A. Tóth, M. Gálová, A. Schleiffer, G. Schaffner, E. Aigner, C. Rupp, A.M. Penkner, A.C. Moreno-Borchart, M. Primig, et al. 2001. A screen for genes required for meiosis and spore formation based on whole-genome expression. *Curr. Biol.* 11:1001–1009. http://dx.doi.org/10.1016/S0960-9822(01)00274-3

Rabitsch, K.P., M. Petronczki, J.-P. Javerzat, S. Genier, B. Chwalla, A. Schleiffer, T.U. Tanaka, and K. Nasmyth. 2003. Kinetochore recruitment of two nucleolar proteins is required for homolog segregation in meiosis I. *Dev. Cell.* 4:535–548. http://dx.doi.org/10.1016/S1534-5807(03)00086-8

Scherthan, H. 2006. Factors directing telomere dynamics in synaptic meiosis. *Biochem. Soc. Trans.* 34:550–553. http://dx.doi.org/10.1042/BST0340550

Scherthan, H. 2007. Telomere attachment and clustering during meiosis. *Cell. Mol. Life Sci.* 64:117–124. http://dx.doi.org/10.1007/s00018-006-6463-2

Scherthan, H., H. Wang, C. Adelfalk, E.J. White, C. Cowan, W.Z. Cande, and D.B. Kaback. 2007. Chromosome mobility during meiotic prophase in *Saccharomyces cerevisiae. Proc. Natl. Acad. Sci. USA.* 104:16934–16939. http://dx.doi.org/10.1073/pnas.0704860104

Scott-Drew, S., and J.A. Murray. 1998. Localisation and interaction of the protein components of the yeast 2 mu circle plasmid partitioning system suggest a mechanism for plasmid inheritance. *J. Cell Sci.* 111:1779–1789.

Shcheprova, Z., S. Baldi, S.B. Frei, G. Gonnet, and Y. Barral. 2008. A mechanism for asymmetric segregation of age during yeast budding. *Nature.* 454:728–734.

Sikorski, R.S., and P. Hieter. 1989. A system of shuttle vectors and yeast host strains designed for efficient manipulation of DNA in *Saccharomyces cerevisiae. Genetics.* 122:19–27.

Sonntag Brown, M., S. Zanders, and E. Alani. 2011. Sustained and rapid chromosome movements are critical for chromosome pairing and meiotic progression in budding yeast. *Genetics.* 188:21–32. http://dx.doi.org/10.1534/genetics.110.125575

Starr, D.A., and H.N. Fridolfsson. 2010. Interactions between nuclei and the cytoskeleton are mediated by SUN-KASH nuclear-envelope bridges. *Annu. Rev. Cell Dev. Biol.* 26:421–444. http://dx.doi.org/10.1146/annurev-cellbio-100109-104037

Sym, M., J.A. Engebrecht, and G.S. Roeder. 1993. ZIP1 is a synaptonemal complex protein required for meiotic chromosome synapsis. *Cell.* 72:365–378. http://dx.doi.org/10.1016/0092-8674(93)90114-6

Tóth, A., K.P. Rabitsch, M. Gálová, A. Schleiffer, S.B.C. Buonomo, and K. Nasmyth. 2000. Functional genomics identifies monopolin: a kinetochore protein required for segregation of homologs during meiosis i. *Cell.* 103:1155–1168. http://dx.doi.org/10.1016/S0092-8674(00)00217-8

Trelles-Sticken, E., J. Loidl, and H. Scherthan. 1999. Bouquet formation in budding yeast: initiation of recombination is not required for meiotic telomere clustering. *J. Cell Sci.* 112:651–658.

Trelles-Sticken, E., M.E. Dresser, and H. Scherthan. 2000. Meiotic telomere protein Ndj1p is required for meiosis-specific telomere distribution, bouquet formation and efficient homologue pairing. *J. Cell Biol.* 151:95–106. http://dx.doi.org/10.1083/jcb.151.1.95

Trelles-Sticken, E., C. Adelfalk, J. Loidl, and H. Scherthan. 2005. Meiotic telomere clustering requires actin for its formation and cohesin for its resolution. *J. Cell Biol.* 170:213–223. http://dx.doi.org/10.1083/jcb.200501042

Tsubouchi, T., A.J. Macqueen, and G.S. Roeder. 2008. Initiation of meiotic chromosome synapsis at centromeres in budding yeast. *Genes Dev.* 22:3217–3226. http://dx.doi.org/10.1101/gad.1709408

Velmurugan, S., Y.-T. Ahn, X.-M. Yang, X.-L. Wu, and M. Jayaram. 1998. The 2μm Plasmid Stability System: Analyses of the Interactions Among Plasmid- and Host-Encoded Components. *Mol. Cell. Biol.* 18:7466–7477.

Velmurugan, S., X.-M. Yang, C.S.-M. Chan, M. Dobson, and M. Jayaram. 2000. Partitioning of the 2-μm circle plasmid of *Saccharomyces cerevisiae.* Functional coordination with chromosome segregation and plasmid-encoded rep protein distribution. *J. Cell Biol.* 149:553–566. http://dx.doi.org/10.1083/jcb.149.3.553

Velmurugan, S., S. Mehta, and M. Jayaram. 2003. Selfishness in moderation: evolutionary success of the yeast plasmid. *Curr. Top. Dev. Biol.* 56:1–24. http://dx.doi.org/10.1016/S0070-2153(03)01005-6

Voelkel-Meiman, K., S.S. Moustafa, P. Lefrançois, A.M. Villeneuve, and A.J. MacQueen. 2012. Full-length synaptonemal complex grows continuously during meiotic prophase in budding yeast. *PLoS Genet.* 8:e1002993. http://dx.doi.org/10.1371/journal.pgen.1002993

Volkert, F.C., and J.R. Broach. 1986. Site-specific recombination promotes plasmid amplification in yeast. *Cell.* 46:541–550. http://dx.doi.org/10.1016/0092-8674(86)90879-2

Wanat, J.J., K.P. Kim, R. Koszul, S. Zanders, B. Weiner, N. Kleckner, and E. Alani. 2008. Csm4, in collaboration with Ndj1, mediates telomere-led chromosome dynamics and recombination during yeast meiosis. *PLoS Genet.* 4:e1000188. http://dx.doi.org/10.1371/journal.pgen.1000188

Westermann, S., D.G. Drubin, and G. Barnes. 2007. Structures and functions of yeast kinetochore complexes. *Annu. Rev. Biochem.* 76:563–591. http://dx.doi.org/10.1146/annurev.biochem.76.052705.160607

Wu, H., D.F. Ceccarelli, and L. Frappier. 2000. The DNA segregation mechanism of Epstein-Barr virus nuclear antigen 1. *EMBO Rep.* 1:140–144. http://dx.doi.org/10.1093/embo-reports/kvd026

You, J., J.L. Croyle, A. Nishimura, K. Ozato, and P.M. Howley. 2004. Interaction of the bovine papillomavirus E2 protein with Brd4 tethers the viral DNA to host mitotic chromosomes. *Cell.* 117:349–360. http://dx.doi.org/10.1016/S0092-8674(04)00402-7

Yu, H.-G., and D. Koshland. 2007. The Aurora kinase Ipl1 maintains the centromeric localization of PP2A to protect cohesin during meiosis. *J. Cell Biol.* 176:911–918. http://dx.doi.org/10.1083/jcb.200609153

Zakian, V.A., B.J. Brewer, and W.L. Fangman. 1979. Replication of each copy of the yeast 2 micron DNA plasmid occurs during the S phase. *Cell.* 17:923–934. http://dx.doi.org/10.1016/0092-8674(79)90332-5

Zickler, D., and N. Kleckner. 1998. The leptotene-zygotene transition of meiosis. *Annu. Rev. Genet.* 32:619–697. http://dx.doi.org/10.1146/annurev.genet.32.1.619

Zickler, D., and N. Kleckner. 1999. Meiotic chromosomes: integrating structure and function. *Annu. Rev. Genet.* 33:603–754. http://dx.doi.org/10.1146/annurev.genet.33.1.603